

Emplacement mechanisms of contrasting debris avalanches at Volcán Mombacho (Nicaragua), provided by structural and facies analysis

Thomas Shea · Benjamin van Wyk de Vries ·
Martín Pilato

Received: 26 October 2006 / Accepted: 18 September 2007 / Published online: 15 November 2007
© Springer-Verlag 2007

Abstract We study the lithology, structure, and emplacement of two debris-avalanche deposits (DADs) with contrasting origins and materials from the Quaternary–Holocene Mombacho Volcano, Nicaragua. A clear comparison is possible because both DADs were emplaced onto similar nearly flat (3° slope) topography with no apparent barrier to transport. This lack of confinement allows us to study, in nature, the perfect case scenario of a freely spreading avalanche. In addition, there is good evidence that no substratum was incorporated in the events during flow, so facies changes are related only to internal

dynamics. Mombacho shows evidence of at least three large flank collapses, producing the two well-preserved debris avalanches of this study; one on its northern flank, “Las Isletas,” directed northeast, and the other on its southern flank, “El Crater,” directed south. Other southeastern features indicate that the debris-avalanche corresponding to the third collapse (La Danta) occurred before Las Isletas and El Crater events. The materials involved in each event were similar, except in their alteration state and in the amount of substrata initially included in the collapse. While “El Crater” avalanche shows no signs of substratum involvement and has characteristics of a hydrothermal weakening-related collapse, the “Las Isletas” avalanche involves significant substratum and was generated by gravity spreading-related failure. The latter avalanche may have interacted with Lake Nicaragua during transport, in which case its run-out could have been modified. Through a detailed morphological and structural description of the Mombacho avalanches, we provide two contrasting examples of non-eruptive volcanic flank collapse. We show that, remarkably, even with two distinct collapse mechanisms, the debris avalanches developed the same gross stratigraphy of a coarse layer above a fine layer. This fine layer provided a low friction basal slide layer. Whereas DAD layering and the run-outs are roughly similar, the distribution of structures is different and related to lithology: Las Isletas has clear proximal faults replaced distally by inter-hummock depressions where basal unit zones are exhumed, whereas El Crater has faults throughout, but the basal layer is hidden in the distal zone. Hummocky forms depend on material type, with steep hummocks being formed of coherent lava units, and low hummocks by matrix-rich units. In both avalanches, extensional structures predominate; the upper layers exclusively underwent longitudinal and lateral extension. This is

Editorial responsibility: C. Kilburn

Electronic supplementary material The online version of this article (doi:10.1007/s00445-007-0177-7) contains supplementary material, which is available to authorized users.

T. Shea · B. van Wyk de Vries
Laboratoire Magmas et Volcans, Université Blaise Pascal,
Clermont-Ferrand, France
e-mail: b.vanwyk@opgc.univ-bpclermont.fr

M. Pilato
UNAN Centro Universitario Regional del Norte (CURN),
B° 14 de Abril. 49,
Estelí, Nicaragua
e-mail: mmpilato@yahoo.com

M. Pilato
Instituto Nacional de Estudios Territoriales (INETER),
Dirección General de Geofísica. Frente a Policlínica Oriental,
Managua, Nicaragua

Present address:

T. Shea (✉)
Geology and Geophysics Department,
SOEST, University of Hawaii,
Honolulu, USA
e-mail: tshea@hawaii.edu

consistent with evidence of only small amounts of block-to-block interactions during bulk horizontal spreading. The base of the moving mass accommodated transport by large amounts of simple shear. We suggest that contractional structures and inter-block collisions seen in many other avalanches are artifacts related to topographic confinement.

Keywords Flank collapse · Debris avalanche deposit (DAD) · Volcanic spreading · Hydrothermal alteration · Substratum · Structural analysis · Hummocks · Lubricating layers

Introduction

Large-scale terrestrial volcanic slope failures have reshaped volcanoes by generating numerous voluminous debris avalanches with their associated scars. Debris-avalanche deposits (DADs) have volumes ranging from 0.1 to 45 km³, can cover several hundreds of square kilometers, and may travel distances greater than 100 km (Stoopes and Sheridan 1992). Thus, they have the potential to cause human losses directly or through secondary catastrophic events like tsunamis, lahars, or magma release (Siebert 1984; Siebert et al. 1987; Voight and Elsworth 1997). Debris avalanches are poorly understood in terms of genesis and transport but seem to follow certain patterns, occurring on structurally weakened volcanoes and generally triggered by short timescale events. As each volcano is built in a unique geologic context and suffers a combination of weakening processes of different types, duration, and intensities, the detailed “formula” needed to produce such massive failures also varies considerably.

This paper considers two large (>1 km³) collapses of different types giving rise to two debris avalanches of similar run-out. Both were emplaced on a flat landscape, unaffected by topographic barriers or valleys. Detailed study of the surface morphology, lithology, and internal structures of these avalanche deposits yields valuable information on emplacement mechanisms.

Collapse mechanisms relating to Mombacho

Commonly invoked mechanisms for triggering edifice collapses are activation/reactivation of basement faults (Vidal and Merle 2000), surrounding/underlying active rift zones (van Wyk de Vries and Merle 1996a; Day et al. 1999), strike-slip faulting (Lagmay et al. 2000), caldera collapse (Hurlimann et al. 1999), magmatic body intrusions (Bezymianny-type activity defined by Gorshkov 1959; Glicken et al. 1981; Voight et al. 1981, 1983; Siebert et al. 1987; McGuire et al. 1990; Elsworth and Voight 1995;

Donnadiu and Merle 1998; Elsworth and Day 1999; Donnadiu et al. 2001), volcanic/tectonic seismicity (Voight et al. 1983), magma-induced pore pressure increase (Elsworth and Voight 1995), or even variations in local water levels (Bray 1977; Firth et al. 1996; McGuire 1996; McGuire et al. 1997; Ablay and Hurlimann 2000).

Recently, much attention has been given to volcano tectonic gravity-driven processes, such as spreading and slumping, to explain edifice weakening and collapse triggering. The concept of gravitational spreading relies mainly on the effects of a volcano’s weight on the underlying strata and on the edifice itself. It was first described by Van Benmelen (1949) and then used by Borgia et al. (1992) to explain the structural formation of Mount Etna. van Wyk de Vries et al. (1996b, 1997, 2000, and 2003) explored the phenomenon further, demonstrating the relation between collapse, edifice weakening, tectonic faulting, and flank spreading.

Volcanic edifice weakening is largely caused by zones of low strength created under the influence of a hydrothermal system. Hydrothermal activity is defined as hot and pressurized fluid circulation maintained by shallow internal or deeper magma sources, rich in corrosive chemicals; these fluids tend to progressively alter the rocks and increase general pore pressure, inevitably weakening the host edifice (Frank 1983; Carrasco-Nunez et al. 1993; Lopez and Williams 1993; Day 1996; Vallance and Scott 1997; Iverson et al. 1997). Under the influence of gravity, the volcano deforms, destabilizes, and generates a slump that develops into a large flank collapse (van Wyk de Vries et al. 2000; Reid et al. 2001; Cecchi et al. 2004).

Geological context

Regional setting

The Mombacho volcano stands on the Central American Volcanic Front (CAVF), which, in Nicaragua, consists of 21 volcanic centers built in the Nicaraguan depression along a near-perfect SE–NW trending line, with summits separated by distances of less than 30 km (Fig. 1).

Most Nicaraguan Quaternary volcanoes were built over three distinct large-scale ignimbrite deposits: the Malpaisillo, Las Sierras, and Chiltepe shields. The Las Sierras and Chiltepe shields originate from the coalescence of large calderas near Masaya (namely, Masaya, Apoyeque, Jilao, and Apoyo calderas).

The ignimbrites generated by the Las Sierras and Apoyo calderas form the present substratum. The pumice-rich Apoyo ignimbrite overlies the Las Sierras and varies in thickness from a few meters in the northern region of Mombacho to a few centimeters in southern zones. It is

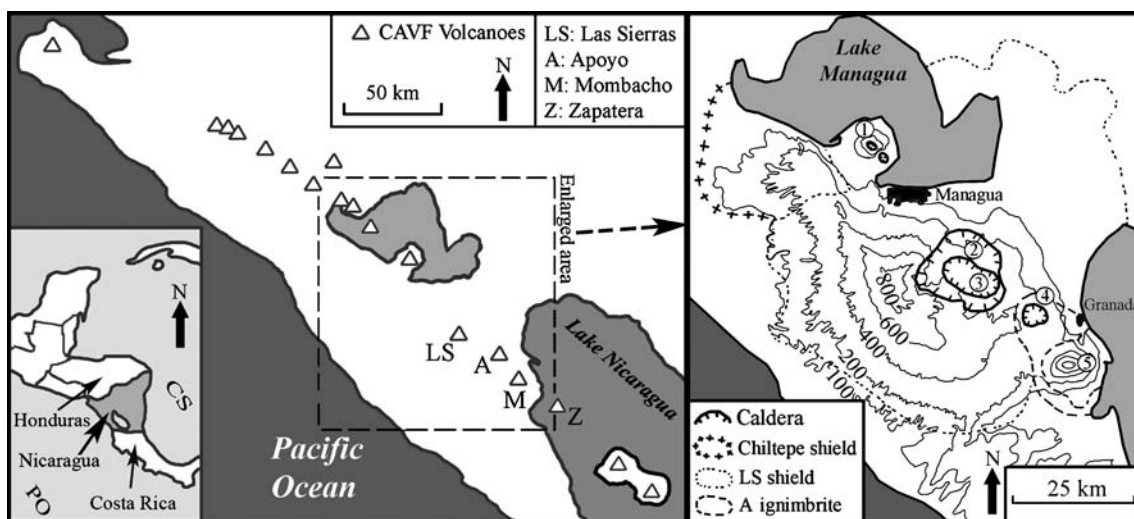


Fig. 1 General map of western Nicaragua with main Quaternary volcanoes (CAVF) and topographic map of enlarged Managua–Granada region. Outcrop distribution of Chiltepe, Las Sierras/Masaya (LS) shields and Apoyo (A) deposit. Modified from van Wyk de Vries

(1993). *PO* Pacific Ocean and *CS* Caribbean Sea in small caption. 1 Chiltepe shield (Apoyeque and Jiloa Calderas), 2 Las Sierras caldera complex, 3 Masaya caldera complex, 4 Apoyo caldera, and 5 Mombacho volcano

likely that Mombacho already existed during the Apoyo eruptions but was smaller than today. Thus, the Apoyo ignimbrite may underlie only the outer rim of the volcano, whereas the Las Sierras may underlie the whole volcano. The extreme east of Mombacho may also be underlain by some lake sediments related to a previously larger Lake Nicaragua.

Mombacho volcano—main features

Mombacho is a 1,345-m-high (a.s.l.) stratocone located roughly 10 km south of the city of Granada, bounded by Lake Nicaragua to the east and by Apoyo Caldera a few kilometers to the north-west. Its plan shape is asymmetrical, and while its summit has been greatly modified, its former symmetry and cone-like geometry are still easily conceivable (photo Fig. 2). The lower parts of its flanks are covered by lava flows equally distributed around the edifice. The rocks originating from Mombacho show discreet variations in composition, from porphyric olivine basalts to hypersthene-augite andesites (Ui 1972).

The drainage system at the base of the volcano shows only young-age gullies carved into the soft layer of underlying Apoyo ignimbrite. The lack of advanced erosion and flat topography enables us to study avalanche deposits mostly undisturbed by surface obstacles (Fig. 2). Uneven topography generally disturbs the avalanche path in other DAD examples, hence, complicating their structure and interpretation (e.g., at Flims, Pollet and Schneider 2004, Dunning 2006; Parinacota, Clavero et al. 2002; Llullaillaco, Richards and Villeneuve 2001; Jocotitlán, Siebe et al. 1992; Tsaticahu, Dunning et al. 2006; and New Zealand’s Falling

Mountain, Acheron, Round top, Poerua rock-avalanches, Dunning 2006). In this case, we examine two lobate debris avalanche deposits showing nearly perfect lateral symmetry, lying on the flanks of Mombacho and on ignimbritic substrata named “Las Isletas” DAD and “El Crater” DAD (respectively, Northern debris avalanche “A” and Southern debris avalanche “B” on Fig. 2) by van Wyk de Vries and Francis (1997).

The summit is carved to the north and to the south by two collapse amphitheatres of dissimilar shapes and volumes, and the original succession of thin andesitic–basaltic lava flows and scoria within their scars is still clearly visible. A third avalanche deposit outcrops south-east of Mombacho (here named “La Danta” DAD, “C” in Fig. 2), although its corresponding scar is hidden by later eruptive products (see also “Additional material 3”). Lava units can be traced to several vents; thus, Mombacho has had multiple eruptive centers, although only three are observed today. Moreover, the edifice is surrounded by many small cinder cones, domes, and explosion craters, testifying to a complex eruptive history. Today, minor fumarolic activity occurs at a few points near the three craters and within the two amphitheatres.

One of the most interesting characteristics of Mombacho is its complex faulting system (Fig. 2), an association of normal, thrust, and strike–slip faults, which share different origins. The majority of strike–slip faults are radial to the volcano, cutting from summit to base. Other strike–slip faults associated with regional tectonics are found south of the volcano, near the Ochomogo fault zone. Their major orientations are close to regional trends (van Wyk de Vries 1993), with N045E dominant. Thrust faults occur in

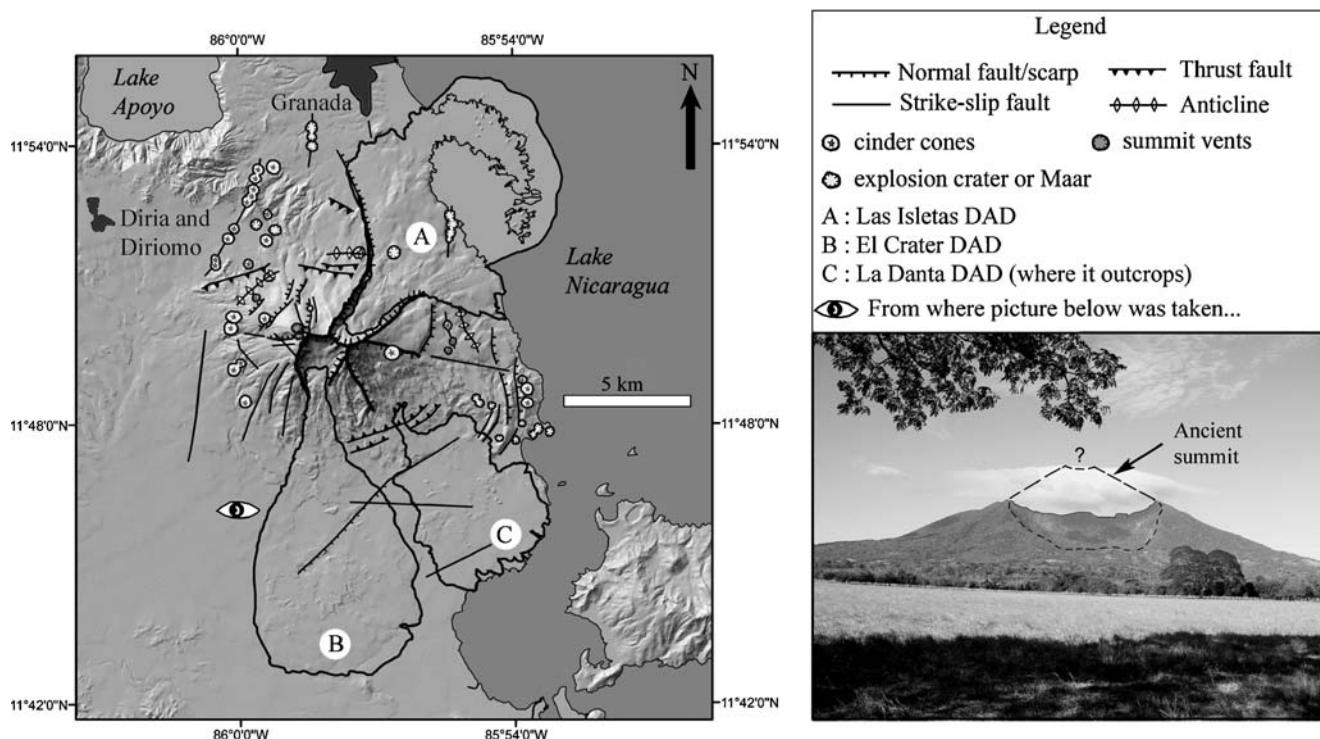


Fig. 2 Ten-meter resolution digital elevation model of Mombacho (source: INETER) with the three DADs and major structural features. *On the right*, photograph of southern collapse amphitheater and inferred former edifice geometry

peripheral zones at the base of the Mombacho. Finally, numerous small normal faults affect the volcano’s flanks, particularly, the western flanks close to the summit.

The majority of the faults are here interpreted as volcano tectonic features rather than regional discontinuities. Radial strike–slip faults are often found associated with lateral edifice spreading (van Wyk de Vries 2003) and thrust faults can likewise form under the influence of volcanic spreading, typically creating peripheral zones of near-horizontal thrusting in the lower parts of an edifice under the influence of the volcano’s own weight. At Mombacho, there is evidence of basal sliding to the north-east and south east (van Wyk de Vries and Francis 1997).

Furthermore, most cinder cones and explosion craters seem to follow thrust zones at Mombacho. This may be because thrust faults associated with edifice spreading facilitate the ascent of magma near the volcano base or because intrusions grow in association with thrusts as lateral sills that break out at the foot of the volcano.

On Mombacho, normal faults are generated by the downward sliding of partially hydrothermally altered steep-sloped zones, and the upper northern flanks may be sliding as well (Cecchi et al. 2004). Such normal fault systems can represent significant hazard sources for nearby populations. In particular, those located in the north-western flanks testify to the flank’s current sliding toward the towns of Diria and Diriomo (Fig. 2).

Las Isletas DAD

General features

The Las Isletas DAD covers a large zone of the north-eastern flank and extends into Lake Nicaragua, forming a cluster of small islands named “Las Isletas” around a curved peninsula (Fig. 3). This formation was first thought to be the result of a large lava flow (Mooser et al. 1958) and is still thought to be the product of a “big volcanic explosion” by the majority of the local population. While the deposit was formed in the pre-Columbian period, archaeological artifacts indicate that it is fairly recent (see “Additional material 1A”).

In plan view, Las Isletas avalanche has a smooth lobate symmetrical shape and displays large bulges on both sides, which we refer to as avalanche wings. The u-shaped scar extends to the base of the volcano, 6.6 km from the summit, with an average slope of 9°. After the 6.6-km point, the topography is almost flat (average 3°), gently sloping into Lake Nicaragua. The deposit’s distal width is 6.1 km and has a run-out distance of 11.9 km from the amphitheater. Correlating this distance with the collapse altitude of about 1,345 m above the base, the height/length ratio is 0.113. The avalanche deposit covers 56.8 km², and its average thickness, deduced from deposit edge heights and map information, is 22 m. Therefore, its calculated volume is

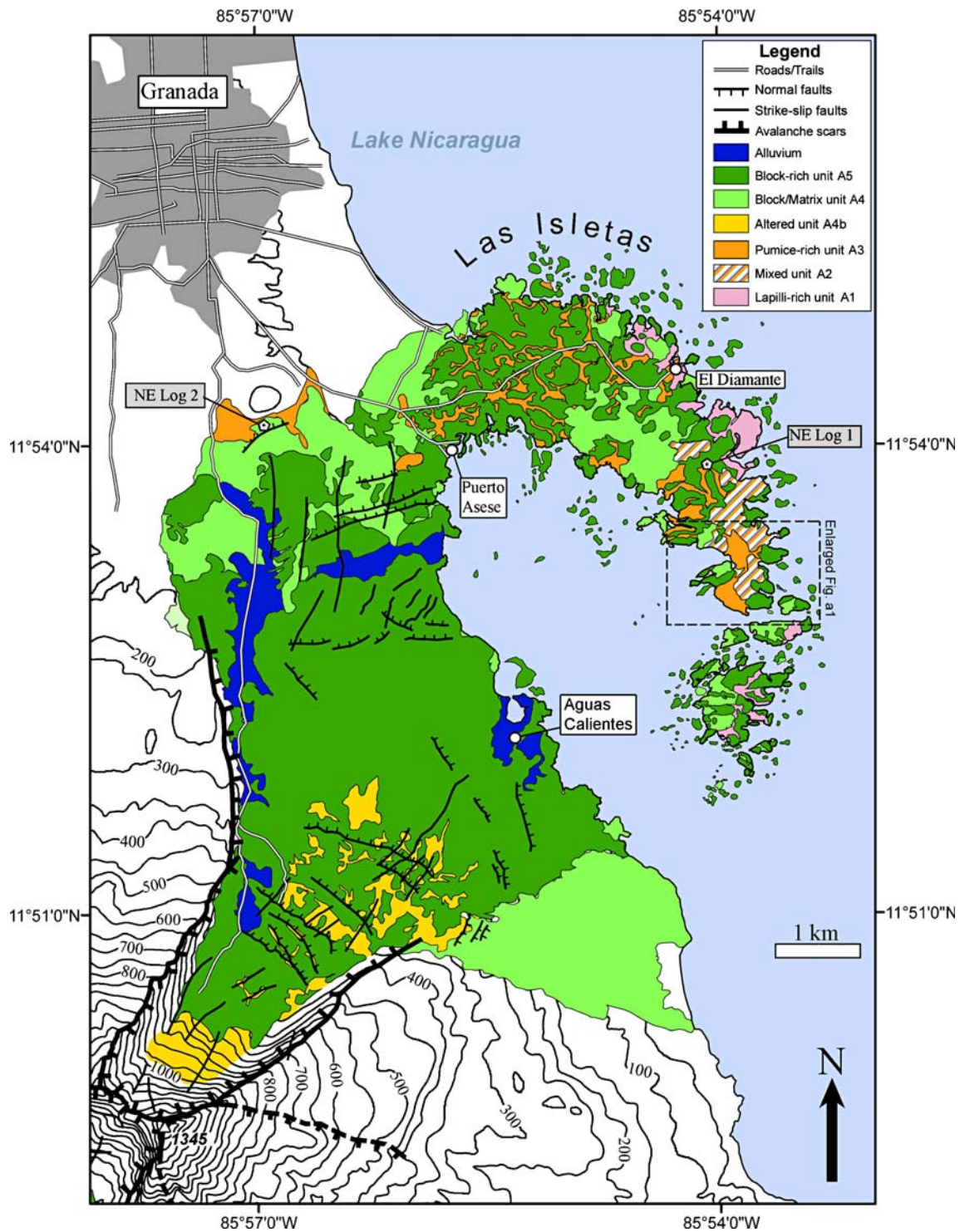


Fig. 3 Lithological and structural map of Las Isletas DAD compiled from field mapping and aerial photographs. Topographic contours every 50 m, Lake Nicaragua coastline at 34 m a.s.l. Area enlarged in Fig. a1 and the two north-western log locations are also represented

around 1.2 km³, whereas the amphitheater is 1.1 km³, implying a volume increase of approximately 10%. There is, however, a non-negligible margin of error in these calculations as part of the avalanche is submerged; thus, volume increase may be higher. The coastal waters are shallow near Granada, so that any prolongation of the

mapped deposit would easily be distinguished. However, on the eastern side of the peninsula where the waters are deeper, the deposit may extend further underwater.

Hummocks are observed on the surface of three zones, namely, the peninsula and at the two side-wings. These tend to disappear toward the amphitheater (Fig. 4a). The deposit

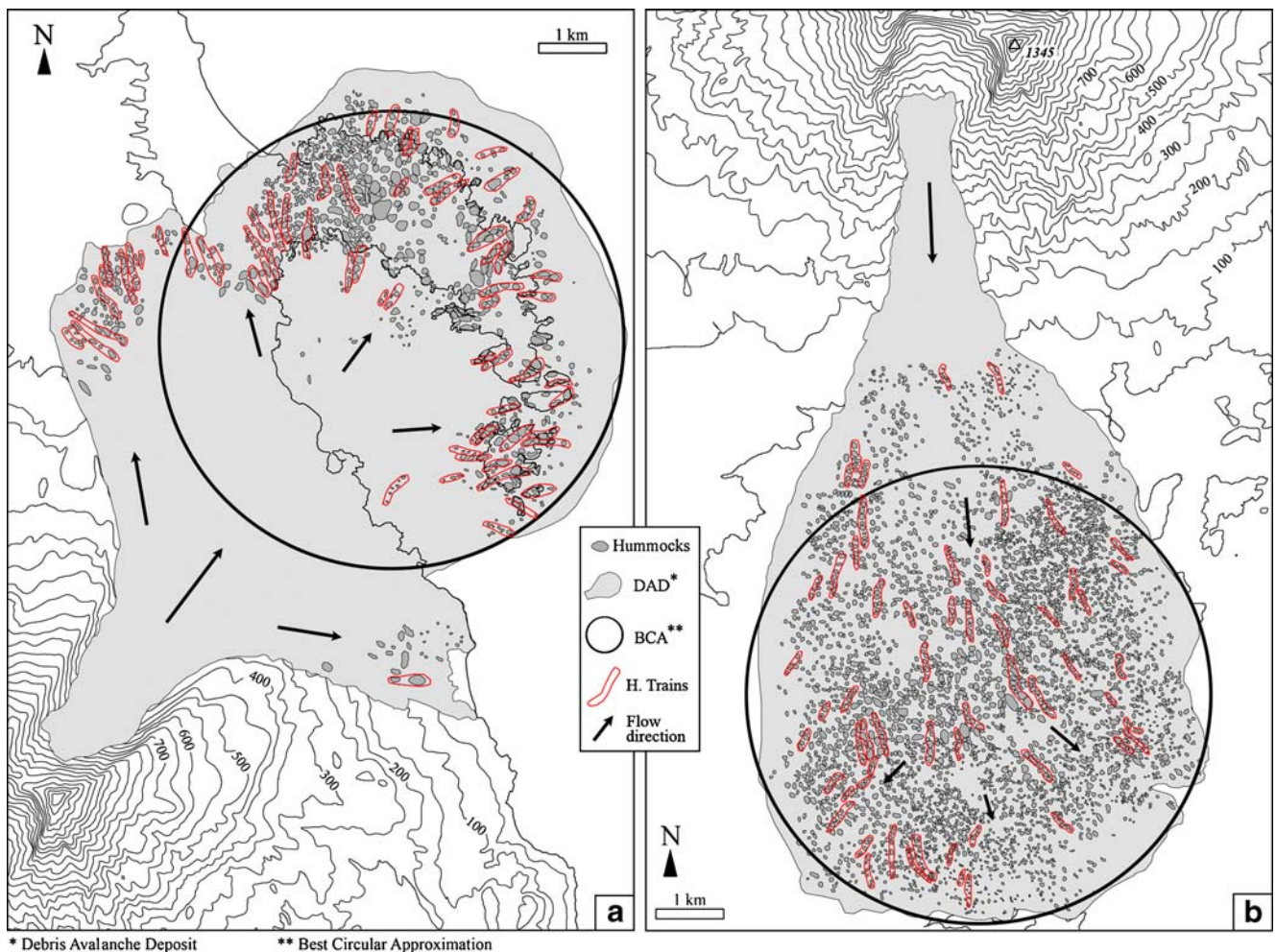


Fig. 4 Map of hummock distribution and hummock trains **a** at Las Isletas DAD hummocks are generally large and concentrated in distal zones and, **b** at El Crater DAD, hummocks are smaller than at Las

Isletas but cover a larger area. Hummock trains at Las Isletas show more variation in flow direction

profile is distally raised (distal thickness > proximal thickness) as shown by the bow-shaped peninsula emerging from Lake Nicaragua after a wide topographic depression extending from the coast to the peninsula.

Numerous explosion craters are observed cross-cutting Las Isletas avalanche particularly near the coast; however, the absence of associated juvenile material shows that the north-eastern zone only suffered light phreatic activity after the collapse.

Main units

In this study, we use a classification based both on lithology and on the allochthonous or autochthonous nature of the units. We distinguish seven key units (A5, A4, A3, A4b, A2, A1, and recent alluvium), which are described following reverse stratigraphical order from top to base (Fig. 3 and log Fig. 6b):

- The *block-rich unit A5* corresponds to the block facies described by Ui (1983), composed mostly of fragments

with sizes ranging from a few centimeters to tens of meters and with a small fraction of matrix. In the distal areas of Las Isletas avalanche, this unit forms high-sloped hummocks and, where the deposit shows no hummocky surface (proximal regions), it is recognizable by its old forest cover. Some local trees exhibit trunk diameters close to 5 m and could date from pre-Columbian periods. The blocks originate from lava flows and are mostly porphyric hypersthene–augite andesites (Ui 1972), dense, non-vesiculated, microlithic-rich, with olivine and plagioclase phenocrysts. They show sharp angular edges, and their surfaces never display hackly surfaces described in some avalanches (Belousov et al. 1999; Komorowski et al. 1991; Clavero et al. 2002; Clavero et al. 2005), which usually testify to block collisions. The transition between the block-rich unit and the block/matrix unit is progressive as the deposits become increasingly enriched in matrix.

- The *block/matrix unit A4* contains blocks of smaller average size, rarely in contact with each other, instead,

generally surrounded by the sand and clay-rich matrix (Fig. 5a). The unit is heterolithic; blocks are composed of basalts, andesitic-basalts and andesites, dense (lava units) or vesiculated (scoria), all of which are variably weathered/altered. Small amounts of pumice are found at the base. Fresh blocks are usually angular but increase in roundness with increasing alteration. Rounded alluvium clasts can be found sporadically in the matrix. In proximal deposits, block surfaces and their surrounding matrix are often more altered by previous fumarolic and hydrothermal activity (*altered block/matrix unit A4b*) than in distal regions, although variations in hydrothermal clays and altered block contents may also occur locally along individual A4 unit outcrops. Perhaps, one of the most crucial observations is that none of the materials are juvenile. This discards the possibility of an eruption-triggered or eruption-associated avalanche. Occasionally, blocks are fractured (jigsaw cracks, Fig. 5b) with their original form preserved, but, like the A5 unit, indications of violent block interaction are absent. The matrix is composed of fine sand and clay-size elements; their respective proportion being correlated with the state of deposit alteration. Figure 6a shows the granulometry of eight samples from this unit. The unit is matrix (<2 mm) and blocks (>64 mm) with lower proportions of gravel materials (2–64 mm). It should be noted, however, that the block percentage is underestimated because of the difficulties of sampling large rock fragments. In this case, each sample consists of 2–3 kg of a mixture of matrix and blocks up to 10 cm in size. High clay contents in the matrix usually indicate that the deposit originates from more hydrothermally altered zones of the edifice. If fragmentation mechanisms during collapse may partly explain the formation of matrix within the moving mass, at Mombacho, the source material was already matrix-rich (fine interstitial ash between scoria within pyroclastic layers and altered/weathered clay-rich material). Even so, at Las Isletas, the matrix content is similar to the block content; it displays an overall good state of material freshness, and soil transformation is constrained to the upper 20 cm of the deposits. Hence, clay weathering in Las Isletas DAD is only a local phenomenon.

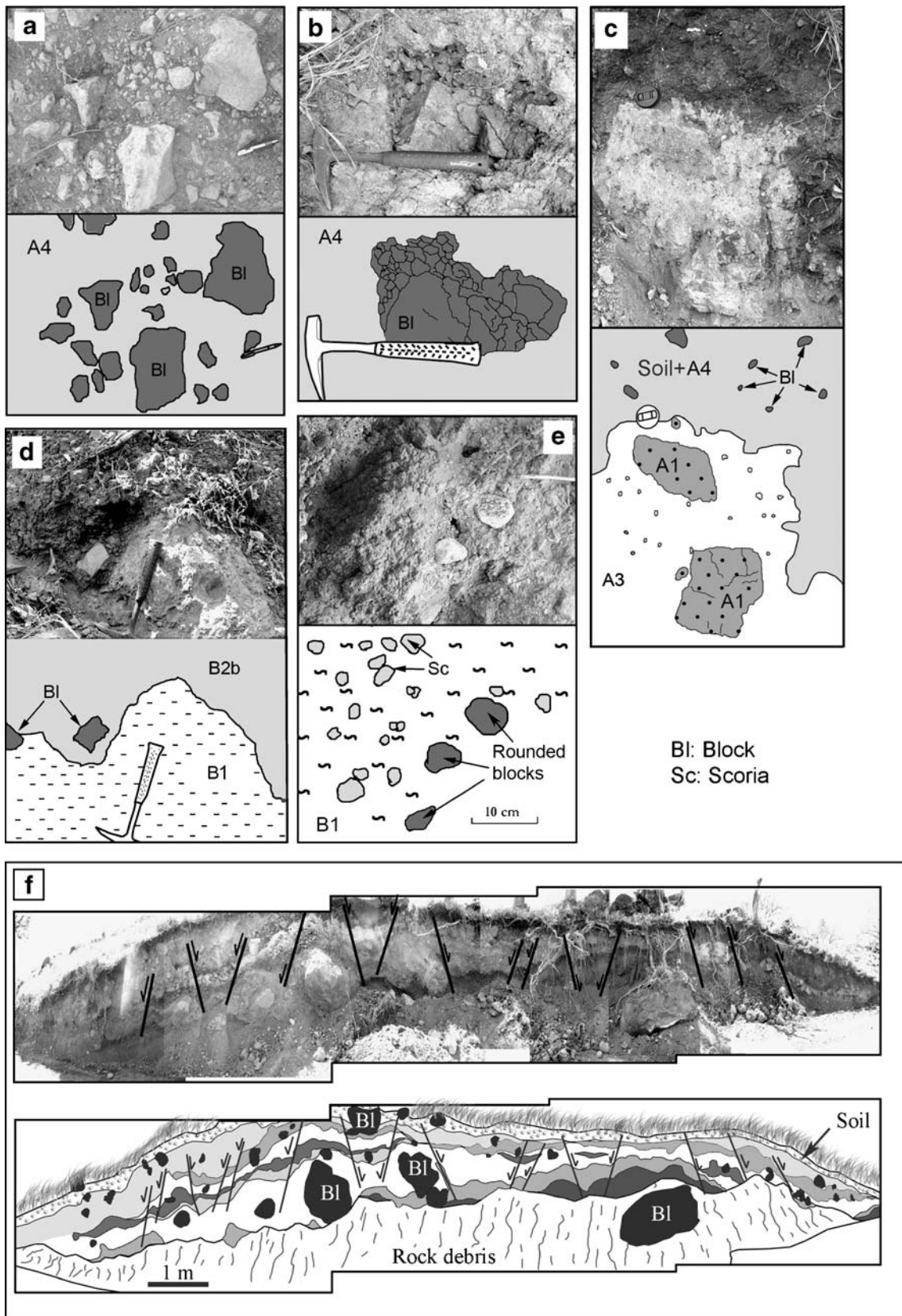
The transition between the upper units (A5 and A4) with the pumice-rich unit A3 is usually clear-cut, although the two tend to interpenetrate each other. Accordingly, fragments of pumice are often found within the base of the A4 formation, and blocks of A4 layer can be included into the upper part of the basal A3 unit. Occasionally, the contact is progressive where pumice clasts are enclosed

into A4 matrix, probably reflecting localized small-scale mixing.

- The *basal pumice-rich unit A3* originates from the Apoyo substrata unit and comprises white rhyolitic pumice, few lithics, individual crystals of amphibole, and occasional fragments of carbonized wood. Pumice ranges in size from a few millimeter to centimeter, rarely exceeding 3–4 cm. The ash-rich matrix is soft and also felsic in composition. Evidence of remobilization in this unit is primarily illustrated by the less angular shape of A3 pumice compared to the ones enclosed in the original Apoyo deposit. This characteristic can be inferred from the weak and easily erodable nature of these rock fragments. The original Apoyo deposit is subdivided into at least two successive episodes and displays alternations of pumice-rich and ash-rich bands, a feature that is not observed in the mobilized A3 unit.

In the western part of Las Isletas debris avalanche, a few outcrops exhibit the contact between the original and remobilized deposit, separated by a 15 cm-thick paleosoil (Fig. 6b). Considering Apoyo subunits are never separated by paleosoils in the original deposit, these outcrops show that part of Mombacho's ignimbritic substratum was undoubtedly remobilized and then transported over a soil formed after the Apoyo ignimbrite, with no apparent erosion. This paleosoil shows almost constant thickness at the scale of the outcrop and forms a near-horizontal contact between A3 and the Apoyo ignimbrite.

- The *basal lapilli-rich unit A1* probably originates from another fraction of the Mombacho substratum, stratigraphically below the Apoyo ignimbrite. It is partly stratified (Fig. 7a), generally competent, and encloses accretionary lapilli ranging in size from 5 mm up to 3 cm. It has low proportions of dacitic pumices (up to 2 cm in length), high proportions of small fragmented lithics, and rare individual crystals of amphibole (Fig. 7b). This unit was originally a product of phreatomagmatic tephra. It can be related to the upper units of the Las Sierras ignimbrite shield, where accretionary lapilli-rich ashfalls are associated with the main deposits. This upper Las Sierras unit is found under the Apoyo pumice to the west of Mombacho, and, considering its presence in the Las Isletas deposit, we infer it should also be under the Apoyo layers near the north-eastern side of the edifice. This unit is not detected in the western part of the avalanche and is first found in the middle of the Isletas peninsula, appearing as extremely fractured and rotated blocks within variable proportions of basal pumice-rich matrix A3. To the east, the formation is clearly contained in the



◀ **Fig. 5** **a** A4 unit of Las Isletas DAD, blocks enclosed in ash to sand size matrix. Pen for scale. **b** Jigsaw-puzzle texture in basaltic block from Las Isletas DAD; core is less fractured than periphery. **c** Mixed unit A2 with fractions of A1 unit within A3 matrix under an upper soil-rich unit (near bones outcrop). Note the sharp contact between the two. **d** Sharp contact between B2b secondary block/matrix unit and B1 extremely altered basal unit. Low block content in both. **e** Close-up of B1 unit; blocks are usually small and have rounder shapes. **f** Hummock outcrop at Las Isletas (peninsula region) made of preserved scoria layers from an ancient cinder cone (shades indicate individual scoria layers). Layers are affected by normal faults; occasionally, they appear as discontinuous lenses testifying to extension suffered during avalanche emplacement. Notice some avalanche blocks are enclosed into the layers regardless of their stratigraphical order. Transport roughly from left to right

pumice-rich unit A3 in the form of decimeter to meter-sized individual blocks. As it is difficult to determine which of the A1 and A3 facies dominates, we use an intermediate unit called “*basal mixed unit A2*” to describe this facies of remobilized substratum (Fig. 5c). Further east, the A1 unit becomes dominant until the basal pumice-rich unit A3 disappears completely. The chaotic blocky nature of the preserved strata is the main feature that indicates transport in the avalanche. This unit occasionally exhibits some beautiful jigsaw cracks within preserved strata (Fig. 7a).

Hummocks

When hummocks are composed of block-rich units, they have high slope angles, sharp summits, and have forest cover. Conversely, when composed of block/matrix units, they have gentler slopes, rounder summits, and are covered by grassy vegetation. In the most easterly zones of the Isletas peninsula, hummocks are seldom formed by basal lapilli-rich deposits and have similar gentle slopes. Occasionally, mounds enclose loose scoria and show even smoother topography. Finally, areas dominated by basal pumice-rich units never show hummocky surfaces; instead, they show depressions where water regularly accumulates during seasonal lake water-level variations. A detailed analysis of the hummocks is given in “Additional material 2A and B.” In general, hummocks show a non-normal positively skewed distribution for length, width, height, and area (Fig. 8c–f and “Additional material 2A”). Individual hummocks show no clear preferred orientation and frequently tend toward circular outline (Fig. 8a, b). Hummock trains, groups of aligned hummocks, coincide with transport direction (Fig. 4a).

Deposit structures

The key to relating Las Isletas deposit and transport style to models of avalanche transport is the multi-scale observation of internal and external structures. The deposits rarely display jigsaw cracks, and hackly textures have not been

observed either on block surfaces or on microscopic particles (Fig. 7e). Voight et al. (1981) and Glicken et al. (1981) described hummocks as successions of horsts and grabens. It is, however, difficult in the field to distinguish these types of structures within the hummocks, generally because of the unstratified nature of the deposits (i.e., no clear deformation markers). Investigation of some hummocks formed by remobilized stratified scoria, similar to those commonly seen near scoria cones on the preserved flanks of Mombacho, clearly shows localized normal faulting (Fig. 5f). Some allochthonous larger blocks are found enclosed within the preserved scoria layers. These particular mounds exemplify the extension systems that form horsts and grabens within hummocky topographies, suggesting dominant extensional dynamics during transport.

This extensional nature is also observed on a larger scale in the form of normal faults affecting the avalanche surface in more proximal regions. Most normal faults show orientations perpendicular (N0135E) to the inferred transport direction (Fig. 3). Others show directions parallel to transport (N045E) but lack significant topographic scarps and are thought to be strike-slip faults. Toward the distal regions, the normal faults become indistinct and are replaced by inter-hummock depressions.

Las Isletas interpretation

The scar is shallow-rooted and cuts the volcano’s flanks down to the base (Fig. 9a). The materials involved are only lightly altered by hydrothermal activity, which indicates that the main factor provoking edifice weakness was probably unrelated to hydrothermalism. No signs of juveniles or any associated juvenile deposit have been found; thus, the avalanche was not associated with a magmatic eruption either.

Probably, the most striking lithologic feature is the presence of part of Mombacho’s substratum at the base of the avalanche deposit. Such a large proportion of sediment could only be *partly* explained by basal erosion mechanisms during transport. Also, there is clear evidence that the topsoil was preserved under the avalanche (i.e., no basal erosion), at least in the western part of the deposit (log Fig. 6b). Hence, as proposed by van Wyk de Vries and Francis (1997), we must examine the possibility of the failure surface cutting through part of the substrata. This has already been observed at Socompa volcano and is interpreted as a consequence of gravitational spreading (van Wyk de Vries et al. 2001). Volcanic spreading can progressively fold and extrude basal sediments, forming a topographic ring-shaped rise around the edifice (Borgia and van Wyk de Vries 2003). This topographic ring is present and still partially visible around northern Mombacho and corresponds to rising anticlines and thrusts (Fig. 2).

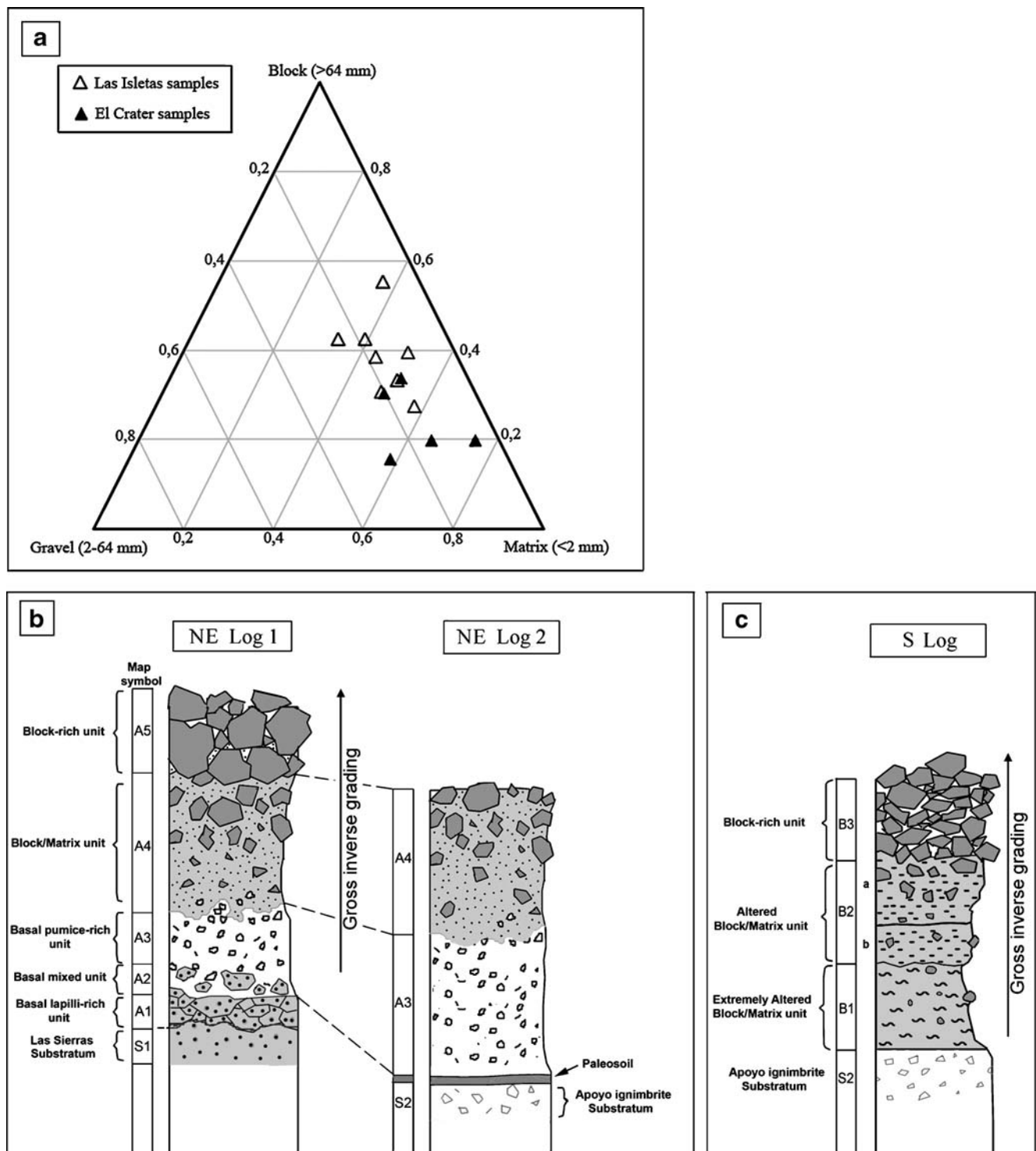
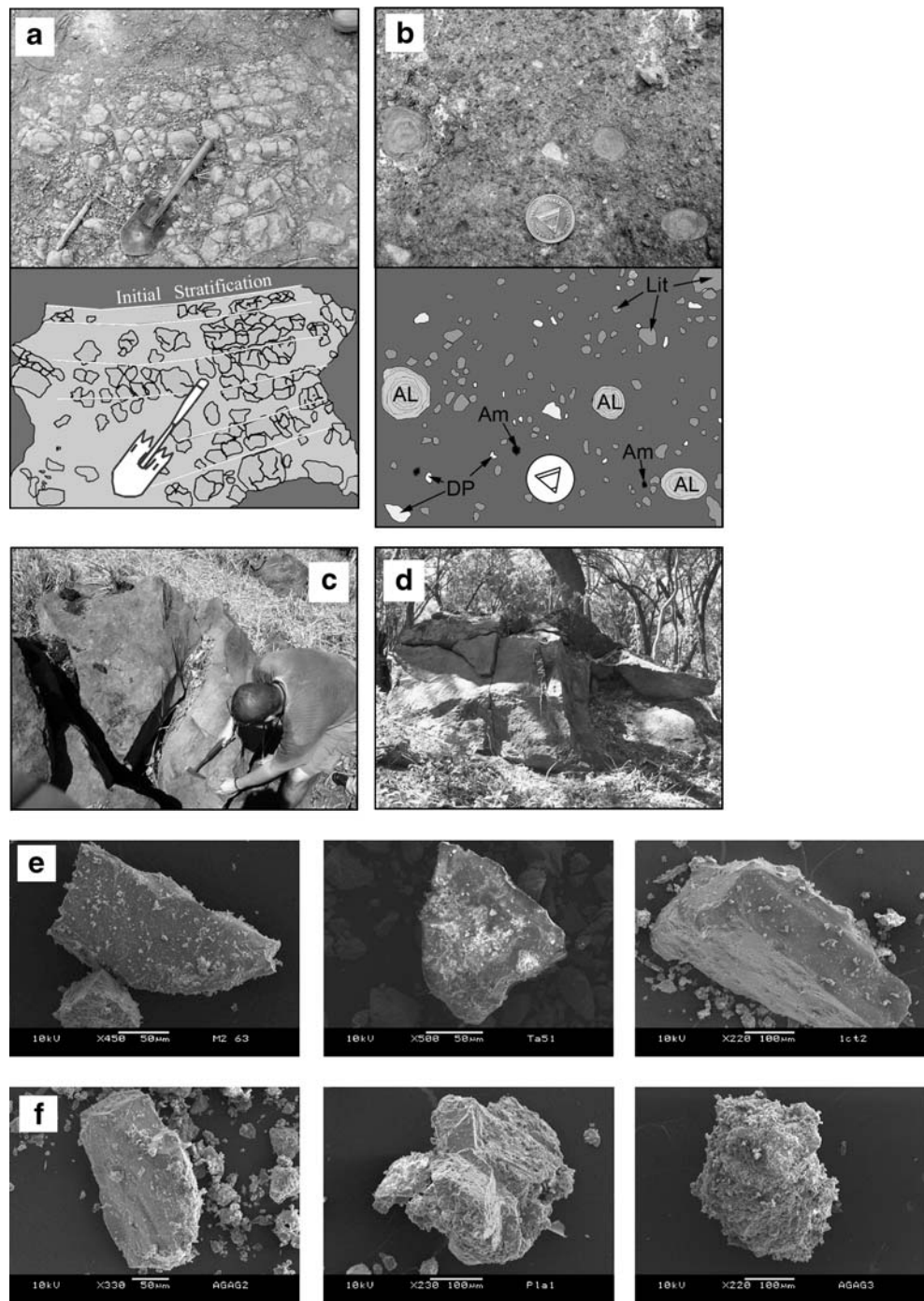


Fig. 6 **a** Ternary diagram of material size for 13 samples (5 from El Crater DAD and 8 from Las Isletas DAD). **b** Comparative stratigraphic logs at Las Isletas DAD (1 and 2; for location, see Fig. 3) and **c** at southern El Crater DAD (location Fig. 9). Vertical thickness not to scale

Importantly, the substratum involved is always positioned at the base of the sequence, and we suggest that basal A3 acted as a lubricating layer. In addition, blocks from units A5 and A4 are almost never found in A3, which leads us to believe the transport did not involve roll-over (accumulation and subsequent burial of blocks at front as

the avalanche moves forward) or turbulent transport mechanisms. The lack of cementation, the absence of evidence of water circulation (e.g., bubbles, water escape structures) in the avalanche units, and the absence of lahar transformation all illustrate the dry character of the collapse.

Fig. 7 **a** Lapilli-rich A1 unit with observable former stratification and jigsaw puzzle fracturing. Shovel for scale. **b** Close-up of Lapilli-rich unit A1. *DP* Dacitic pumice, *AL* accretional lapilli, *Lit* lithics, *Am* amphibole crystals, coin for scale. **c** Large jigsaw-fractured block from Las Isletas DAD; notice the lack of abrasion of shock signs on block surface. Person for scale. **d** Plurimetric fractured block from El Crater DAD; again, no evidence of block–block collision on the block surface. Machete for scale. **e** SEM images of three block/matrix unit A4 samples from Las Isletas DAD. Notice the lack of jigsaw fractures and hackly textures on particle surface and their high angularity. **f** SEM images of three samples respectively from three distinctly altered samples of El Crater avalanche. *On left*, slightly altered particle and, *on right*, highly altered fragment. Notice the clay formation on their surfaces, and again, the lack of jigsaw fractures and hackly textures



The two upper units (A5 and A4) show evidence of original shape preservation, with their main elements being slightly fractured (jigsaw cracks affecting blocks and archaeological remains). In addition, some deposits display a well-preserved paleo-stratification, further supporting a translational, nonturbulent type of transport. Importantly, a general inverse grading is also observed in the deposits, which indicates that segregation may have occurred during motion. The alternating scoria/lava units of the Mombacho

edifice stratigraphy are converted into a distinctive unit grading from block-poor at the base to block-rich at the top.

Two types of hummocks are observed: One group is formed by large block concentrations (A5) and are generally steep and conical. The other is formed by smaller blocks and matrix (A4), with rounded, more gentle topography (see “Additional material 2A” for detailed hummock descriptions and statistical analysis). The difference in shape can be interpreted in terms of material properties, where final

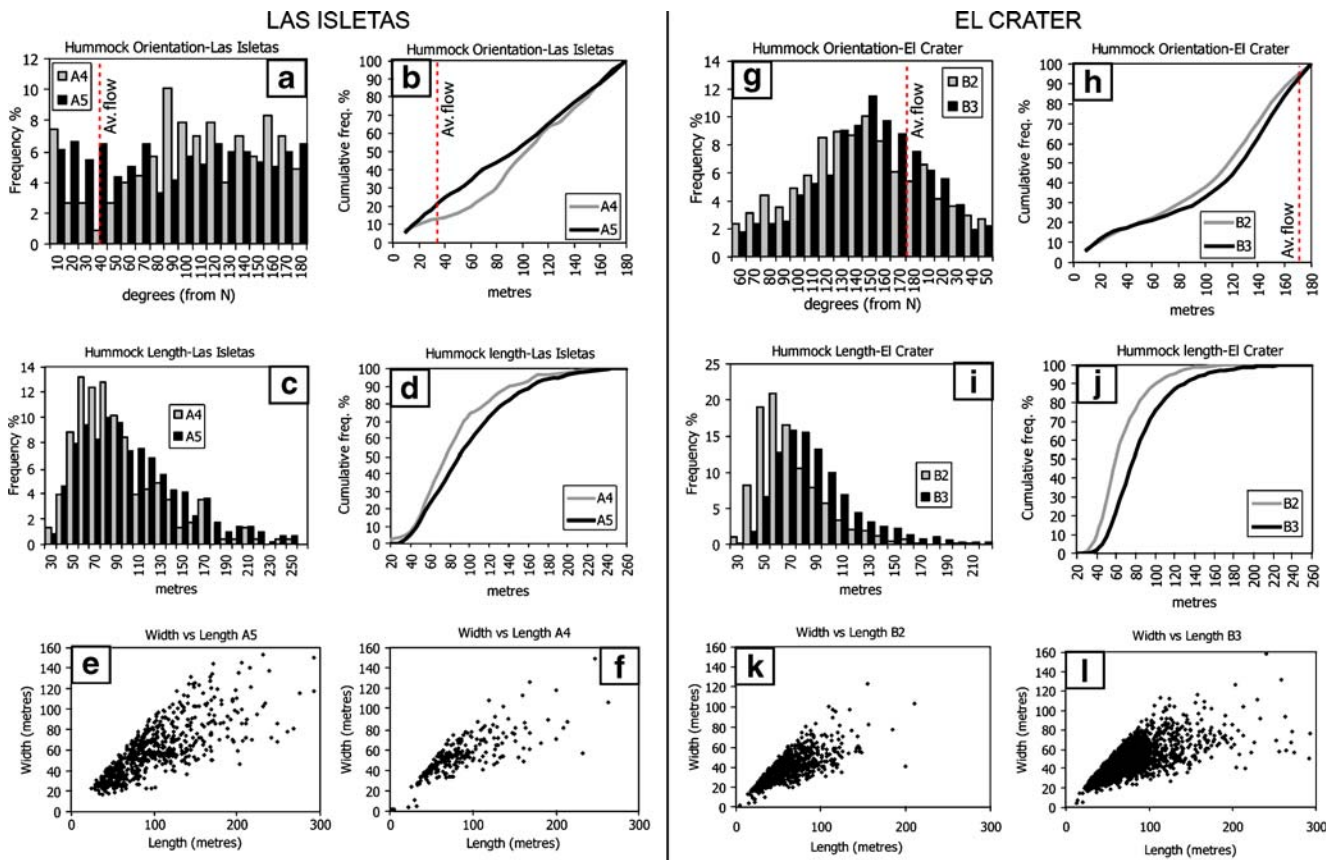


Fig. 8 Las Isletas (a–f) and El Crater (g–l) hummock statistical analysis. Histograms and corresponding cumulative frequency curves of A4/A5 and B2/B3 hummocks for orientation (a, b, g, h), length (c, d,

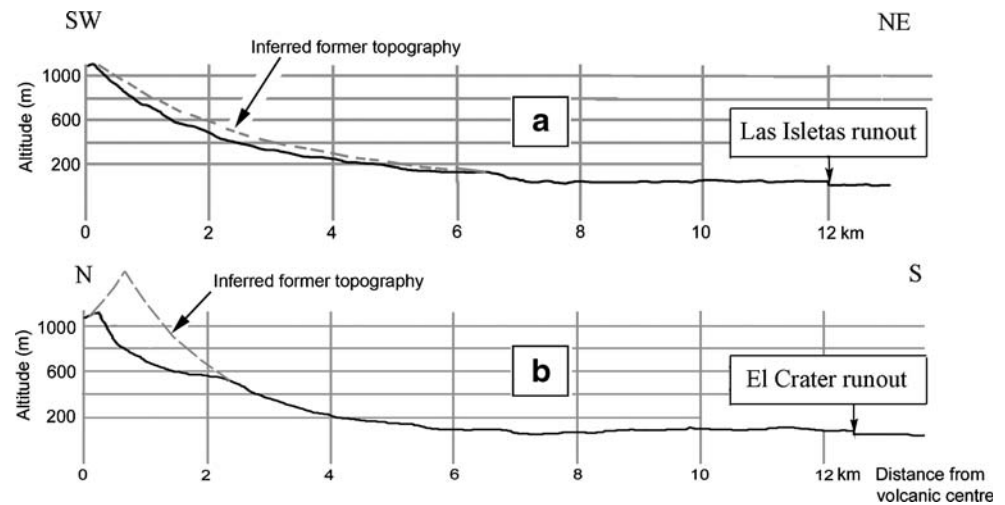
i, j). Width vs length plots for both avalanches (e, f and k, l). Red lines on orientation plots show main directions of avalanche flow. Note that orientation scale for g is shifted toward the left for clarity reasons

deformation and, hence, slopes may be controlled by factors such as cohesion and angle of internal friction. Our measurements show that hummocks formed dominantly by the matrix A4 tend to be smaller in size than those formed by the blocky A5 (Fig. 8c, d). More generally, the distribution of hummock length, width, area and height follows a nonnormal positively skewed distribution that could relate to the separation of hummocks into progressively smaller units (i.e., where smaller mounds form at the expense of larger ones). The length vs width plots (Fig. 8e, f) show that hummocks are frequently circular at their base. On the other hand, their individual orientation is more random (Fig. 8a, b). As an avalanche spreads in multiple directions, hummock orientation could reflect these changes. Accordingly, hummocks close to the center will be elongated parallel to flow, whereas those closer to the edges will be elongated oblique. If flow directions significantly differed from west to east at Las Isletas, hummock orientations would also vary. This could partly explain the absence of a clear, dominant orientation. If we focus on aligned groups of hummocks (hummock trains) rather than individual units, trends appear (Fig. 4a). These mark a transport-parallel

direction and illustrate west to east variations. Hummock reorientation upon entrance of the avalanche into Lake Nicaragua is yet a third possible explanation for this. Hummocks would be reoriented perpendicular to flow if sufficient compression (here, the resisting force generated by the Lake) was applied. However, hummock trains indicate otherwise, and at every scale, structural analysis reveals an avalanche surface affected by extension.

Typical compressional features, such as thrust faults, are not observed, whereas normal faults and extension-related structures such as hummocky surfaces are common in the upper layers of Las Isletas deposit. Analysis of the basal layers is trickier as one of them (basal pumice-rich unit A3) is loose and soft, and generally unstratified. Likewise, the basal lapilli-rich A1 unit is too often found disaggregated and enclosed in A3 fine matrix (Fig. 5c). This could simply result from a stretching and boudinage process occurring during transport as a consequence of two different rheological behaviors (i.e., A1 more competent). Finally, the absence of faults toward distal regions probably reflects fault zone transformation into wider inter-hummock topographic depressions (grabens) as the avalanche spread out.

Fig. 9 Topographic profiles along Las Isletas avalanche (a) and El Crater avalanche (b) with inferred former edifice shape. c Interpretative sketch of failure locations and mechanisms for Las Isletas (substratum folding and extrusion) and El Crater (hydrothermally altered core)



El Crater avalanche

General features

The El Crater event may be historic, as there are accounts of a disastrous event in 1570 (see “Additional material 1B and C”). The amphitheater left by the southern El Crater collapse (1.25 km^3) is deeper than that of Las Isletas. Its scar extends to about 2.3 km from the summit with an average slope of 19° and further gives way to the remains of the volcano’s southern flanks, which extend 6 km away from the summit (average slope, 6°). Finally, the flanks give way to the Apoyo ignimbrite substratum, which slopes gently to the south ($<3^\circ$).

The avalanche deposit has a lobate, symmetrical plan shape (Fig. 2 and Fig. 10), covering an area of 49.5 km^2 and reaching a distance of 12.4 km with a central width of 6.5 km. Correlating its run-out distance with the inferred collapse altitude (1,345 m) yields a H/L ratio of 0.108.

The calculated collapse volume depends on initial hypotheses. The present topography taken from a 10-m resolution digital elevation model shows that if a previous cone-like summit existed, it was centered where the current amphitheater is. Thus, we might need to add a certain volume assumed to represent the ancient summit (Fig. 2). This additional volume can be approximated to a truncated and cratered cone. Using a crater type (diameter and depth) similar to other Nicaraguan volcanoes of comparable height (Momotombo, San Cristobal, Concepcion), we subtract a crater volume from the truncated cone and, finally, obtain an additional 0.5 km^3 , giving a final collapse volume of 1.75 km^3 . Given this hypothesis, the fall height rises to 1,500 m, and accordingly, H/L rises to 0.12.

The deposit shows a mostly uniform profile (distal thickness = proximal thickness) with an average thickness of 38 m (evaluated using topographic profiles), leading to a

calculated deposit volume of 1.88 km^3 . Thus, the DAD volume was clearly greater than the southern amphitheater alone (almost 40% volume increase from 1.35 km^3) and is marginally larger than the inferred total collapsed edifice (8% volume increase from 1.75 km^3).

A hummocky surface covers most of the deposit, with a much larger area in proportion to that of Las Isletas (Fig. 4b). Notably, the hummocks are not exclusively restrained to distal regions.

Unlike Las Isletas avalanche, El Crater deposit is not affected by explosion craters. A large scarp of N045E orientation is visible in its central regions aligned with a set of Lakes (Las Lagunas scarp, Fig. 10), interpreted as a regional discontinuity associated with the Ochomogo fault zone (van Wyk de Vries 1993). The small topographic jump generated by this fault scarp is draped by the deposit.

The avalanche’s underlying substratum is the Apoyo ignimbrite deposit, which forms a flat topographic plain around the edifice. Like Las Isletas avalanche, the lack of significant topographic barriers explains the simple geometric shape of El Crater avalanche.

Main units

The main units of El Crater deposit can be subdivided into four formations, from top to base (Figs. 6c, 10):

- The *block-rich unit B3* also corresponds to the block facies of Ui (1983), composed mainly of fragments with sizes ranging from a few centimeters to 4–5 m and with a small proportion of matrix. On average, blocks are smaller than in Las Isletas avalanche, and overall, B3 is thinner than the northern A5 unit. Blocks have the same compositions as in Las Isletas, which is no surprise, as lava flows were quite equally distributed around the edifice. They also display sharp/angular

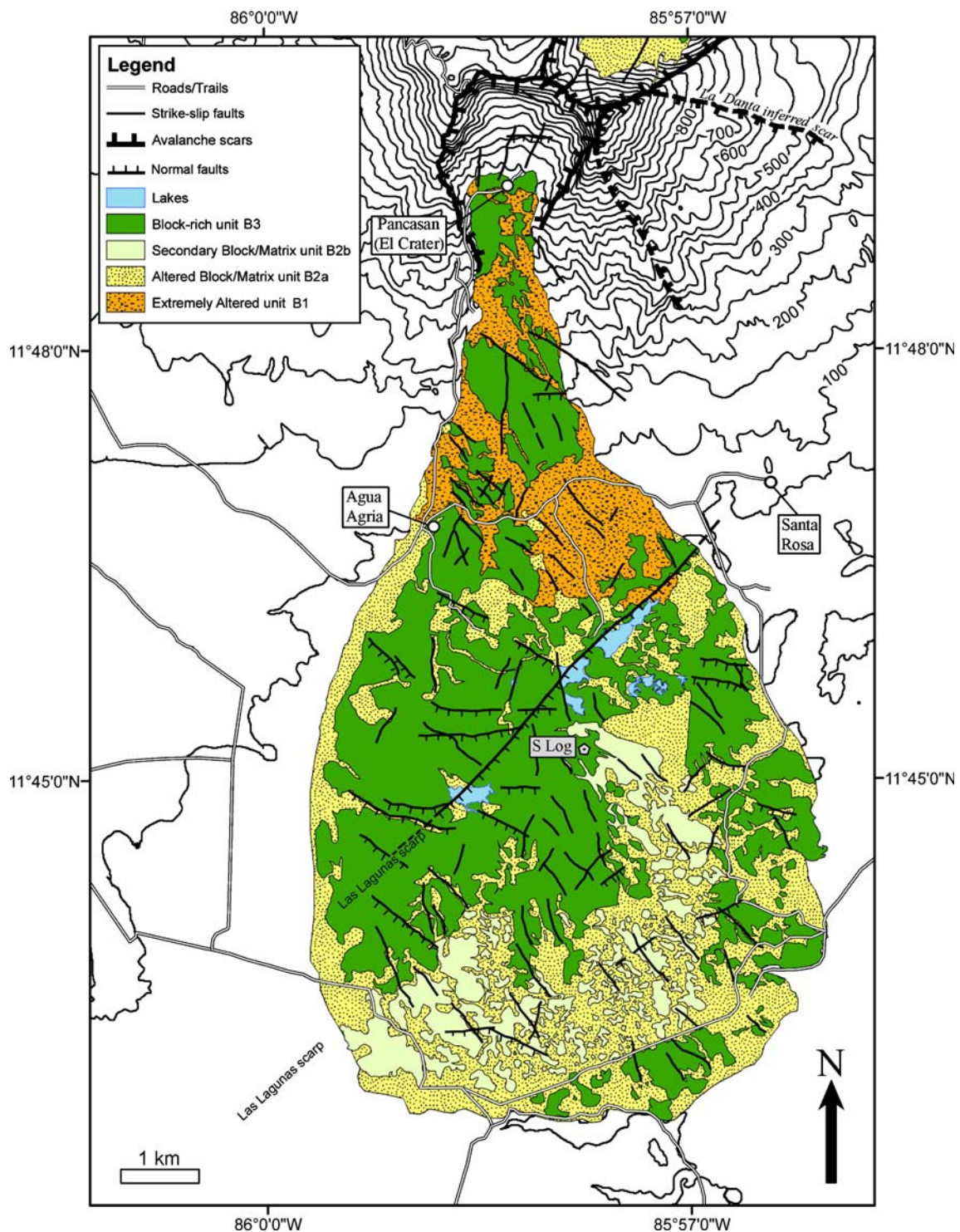


Fig. 10 Lithological and structural map of El Crater DAD compiled from field mapping and aerial photographs. Topographic contours every 50 m; Lake Nicaragua coastline at 34 m a.s.l. Southern log location also represented

edges and faces that lack signs of collision (Fig. 7d). A dominant proportion of the blocks have hydrothermally altered surfaces and show evidence of fluid circulation. The transition between the block-rich unit B3 and the altered block/matrix unit B2 is progressive as the proportion of matrix increases downward.

– The *altered block/matrix unit B2a* encloses blocks of much smaller size (rarely larger than 30 cm), fully surrounded by an ash- and clay-rich matrix. The unit is also heterolithic, and block surfaces are often altered to orange/reddish clays that, at their most developed, also fill vesicles in clasts. Unlike the

northern block/matrix unit A4, the deposits contain significant proportions of red inner-cone facies scoria that display a more advanced state of alteration. The matrix is composed of the same clays as the block surfaces, and their predominance indicates that the units probably originate from the more hydrothermally altered central core of the edifice. None of the materials are juvenile. Granulometry measured in five samples from this unit shows a dominant proportion of matrix (<2 mm) over blocks (>64 mm) and gravels (2–64 mm), respectively. Overall, samples from El Crater enclose smaller clasts than those of Las Isletas (Fig. 6a). Occasionally, blocks are fractured with jigsaw cracks, having their original block form preserved.

- The *secondary block/matrix unit B2b* is quite similar to the B2a unit, except that its block content is even lower. Morphologically, the zones dominated by this unit form hummocks with low slopes and rounded summits. In both cases (B2a and B2b), the transition to the basal B1 unit is sharp, although the layers tend to interpenetrate each other, in a similar manner to that observed in Las Isletas avalanche (Fig. 5d), between the block/matrix unit A4 and the basal pumice-rich unit A3.
- The *extremely altered block/matrix unit B1* encloses exclusively altered basaltic/andesitic blocks and scoria within a clay-rich matrix. The particles are generally more rounded than those of the previous units (Fig. 5e). The matrix is composed of orange/reddish to white clays of hydrothermal origin, whose nature depends on the original material composition and on that of the circulating fluids themselves. This facies is interpreted as the innermost fraction of the edifice core, more subject to alteration. It is the lowest unit of El Crater sequence, forming the entire deposit thickness in proximal areas and found at the base of other units in more distal regions. On the geologic map (Fig. 10), B1 is seen exclusively in proximal areas simply because, in more distal areas, it is covered by B2 and B3 and rarely outcrops.

Hummocks

Using orthophotos, we mapped more than 2,900 hummocks and measured them for length, area, and orientation. Unfortunately, no available detailed topographic map covers the southern avalanche; thus, hummock height could not be measured. Results are plotted along with those from Las Isletas to allow clear comparison (Fig. 8g–l). Histograms and plots show that there is a dominant hummock orientation at 140° (Fig. 8g, h). The matrix hummocks are smaller (Fig. 8i, j) and shorter than the block unit ones.

Smaller hummocks in both units are more rounded, and many have circular bases (data concentrated along the length = width line in Fig. 8k, l). Flow-parallel hummock alignments are also distinguished, as at Las Isletas (Fig. 4b). For a full description of hummock morphology, see “Additional material 2B.”

Deposit structures

Similar to Las Isletas avalanche, the deposits seldom exhibit jigsaw cracks. Evidence of extension dynamics during deposit has also been found in the southern avalanche, where original scoria stratification is preserved, and is cut by sets of normal faults similar to those observed at Las Isletas (see Fig. 5f).

At a larger scale, the avalanche surface shows a larger number of normal faults/fractures than Las Isletas, most of them located in the central part of the deposit, perpendicular to the inferred transport direction. Other faults/fractures show orientations (N0135E) and (NO45E) and, probably, have a strike–slip component. Thus, similar to Las Isletas, structures demonstrate a surface generally affected by extension mechanisms, with no evidence of compression.

El Crater interpretation

The southern bowl-shaped scar cuts the edifice deeply to uncover an altered core, and although it does not reach the base like the northern failure plane (Fig. 9b), the void left by the collapse is greater.

The deposits contain a larger proportion of scoria that, because of high vesicularity, may have allowed easier fluid circulation and, thus, enhanced alteration. In general, materials involved are highly altered by hydrothermal activity, which points to hydrothermalism as the main cause of edifice weakness in the southern zone. The particles are more rounded in the most altered units, as weaker materials facilitate transport-related abrasion/erosion.

The lack of juveniles discards an eruption-triggered or eruption-associated collapse mechanism. Avalanche blocks lack evidence of collision, which testifies to a transport devoid of violent interactions between the main components. This does not mean, however, that violent block interactions did not occur during collapse before the bulk of horizontal transport. If collisions are created by compressional waves, which themselves are generated by topographic obstacles, then their absence at Mombacho could be simply related to the smooth topography. Blocks may also be cushioned during transport if their proportion is lower than the surrounding matrix, which may prevent them from colliding.

Taken as a whole, El Crater avalanche has a higher content of fine materials than Las Isletas (Fig. 6a). We

interpret this feature as being the consequence of primary weakening/fracturing and clay transformation during hydrothermal circulation, which may have further facilitated the break-up of the material during collapse. The source material of El Crater avalanche was, thus, already rich in what would later form a significant fraction of the deposit matrix.

When original strata are preserved in the deposits, they are always cut by sets of normal faults with nearly constant dip ($>50^\circ$). These features correspond to a dominant extensional deformation mechanism and confirm the horst and graben model of hummock formation suggested by Voight et al. (1981) and Glicken et al. (1981).

Compared to Las Isletas debris avalanche, El Crater hummocks made by block-rich units (B3) are larger in size, show lower slopes, and rounder summits. The ones formed by block/matrix units (B2) have even gentler slopes and are sometimes hard to distinguish in the topography. As noted previously, the extent of the hummocky topography on El Crater deposit is much greater than in Las Isletas. Hummocks are dominantly oriented $140\text{--}150^\circ$, which is close to the 170° main transport direction of the avalanche. The $20\text{--}30^\circ$ difference may be explained either by a slight reorientation of some hummocks during stoppage or could simply result from small asymmetries in flow directions. Accordingly, most recurrent orientations represent the main flow direction, and less frequent values, probably, correspond to hummocks closer to the edges, oblique because of lateral avalanche spreading (Fig. 8g, h). Hummock alignments indicate that the avalanche surface was mostly affected by an extensional regime parallel to transport at least during their formation. Conversely, if the deformational regime parallel to the mass movement was strongly compressional, hummocks and hummock trains would be mostly elongated perpendicular to the inferred transport direction. Similar to Las Isletas, hummock size and area follow a positively skewed distribution, which supports progressive break-up of hummocks into smaller and smaller components.

Although the Granada archives (see Additional material 1C) state that heavy rainfall preceded failure, no evidence of high water contents (e.g., avalanche transforming into lahar) has been found. Hence, rainfalls associated with the abnormal seismic activity might have been the triggering factor, without playing a significant role during transport. Although El Crater avalanche is quite different from Las Isletas deposit and did not involve substratum, we may infer that the more altered unit (B3a) probably acted as a weaker, lubricating layer comparable to the A3 pumice-rich unit. It may be argued that A3, being ash-rich (ignimbrite ash), should contain finer material than B1. However, the unit B1 suffered extreme hydrothermal alteration before collapse. Hence, a high proportion of material was transformed into fine clays comparable to A3

in size and was probably fragmented more efficiently during or before transport. Accordingly, the interpenetrating transition between B2 and B1 indicates the ductile nature of B1, which, we infer, served to lubricate the avalanche base.

Another important observation is the absence of blocks in the basal B3a unit, indicating again the lack of roll-over or significant turbulence during transport. Furthermore, a gross inverse grading similar to that in Las Isletas DAD is observed in the whole of the deposit, from block-free units at the base to dominantly block-rich units at the top. Consequently, a separation process may be invoked where either small particles migrate downward during transport or blocks migrate upward but without total disruption of the original layering. Dynamic fragmentation (Davies et al. 1999; Davies and McSaveney 2002; Smith et al. 2006) or passive fragmentation associated with simple material-loading during failure are plausible mechanisms for this separation.

Discussion

We provided two well-preserved nonsynchronous examples of debris avalanches originating from the same volcanic edifice. The presence of smooth topography around Mombacho allowed them to spread freely, and the young age of both avalanches allows excellent conditions for field study. Eruptive activity and generated products associated with large-scale volcanic flank failure adds further complications when attempting to characterize surface structures. Thus, at Mombacho, the lack of topographic complication, the noneruptive characteristic of the collapse, and the absence of advanced erosion for these avalanches offer an unprecedented setting for comparing the emplacement and transport of two contrasting mass movements. Identifying mechanisms capable of generating structural/internal differences and similarities then becomes possible.

The two debris avalanches described are similar in many aspects:

- Neither was influenced by topographic irregularities, and both have lobate, unrestricted spreading geometry.
- Neither displays any magmatic activity related to the collapse.
- Neither seems to have held significant water during transport and deposition, even when emplaced into or over water saturated land.
- Both were deposited on top of the Apoyo ignimbritic unit.
- Both display normal faults and extension-related structures that together support a horst-graben model proposed for the formation of hummocks.

- No observed thrust faults, clastic dykes, or hackly textures.
- Rarely observed jigsaw cracks.
- Both had a lubricating layer for transportation. Such layers may have been fluidized by media such as air, gas, or water. However, no injections or clastic dykes (i.e., evidence for vertical gas/fluid escape) were seen in the deposits as in other avalanches (e.g., Parinacota, Clavero et al. 2002).
- Neither holds evidence of particle rotation or roll-over mechanisms, indicating that the mass “slid” rather than rolled or flowed.
- In both avalanche deposits, block-rich units tend to form steep slopes in hummocks and, conversely, finer matrix materials form more gentle mounds. This feature confirms that surface materials behave like dry granular material (as opposed to wet), forming slopes determined by material type and size (angle of internal friction and cohesion).
- Both have gross inverse grading and evidence of extreme stretching, boudinage, and thinning.

Collapses show differences in:

- Their *content of altered material*: El Crater contains a higher proportion than Las Isletas.
- Their *content of substratum material*: Las Isletas DAD contains a significant proportion of Las Sierras and Apoyo ignimbrite, whereas substrate is negligible in El Crater DAD.
- The *shape of the amphitheater*: Shallow rooted and extending down to the base of Mombacho in the case of Las Isletas and deep-rooted and bowl-shaped in the case of El Crater.
- The *hummocky surface* forms a distal arc, well marked in topography, in Las Isletas deposit, whereas it covers a greater area (most of the avalanche surface), and is poorly marked in the topography at El Crater. This confirms that the overall proportion of fine material in El Crater was greater than that at Las Isletas, as finer materials tend to form smaller hummocks with gentler slopes.

Collapse mechanisms

In the north, we believe failure was similar to that of Socompa (van Wyk de Vries et al. 2001), where the failure surface cuts the volcano down to the base, and where large proportions of substratum (Apoyo ignimbrite and the Lapilli unit) were directly involved. Therefore, like van Wyk de Vries and Francis (1997), we can invoke gravitational spreading as the main cause of the Las Isletas

collapse, where volcano weight caused deformation of the ignimbrite substratum. The extruded substratum was then cut by the failure surface. Studies on the Socompa and other volcanoes have shown that spreading can create major subhorizontal thrust faults at the base of the edifice. This set of basal faults may have progressively pushed the extruded substratum toward the north-east and created a surface of weakness.

In the south, the high content of extremely altered material (transformed into clays) provides evidence that the rock mass suffered intensive hydrothermal alteration before the collapse. The amphitheater left behind has a smaller surface area than Las Isletas and confirms edifice core alteration as the main cause of the failure. If hydrothermal alteration alone can be considered over time a major weakening factor, it is difficult to believe it “triggered” the southern collapse, instead, historical archives infer that the trigger to this avalanche may have been continuous swarms of seismic activity concluded by an earthquake in 1570.

Mode of transport

If we consider the hypothesis of a moving rock mass that exclusively suffers complete shearing from top to base (as opposed to a plug-flow model where shear is concentrated at the base), then the resulting deposits should show corresponding tectoglyphs (sheared jigsaw-cracked blocks for example), and the topmost layer of the initially slope-parallel stratigraphy should have traveled further than the base layer. No such features are observed in Las Isletas and El Crater avalanches, and the basal units (A1–A3 at Las Isletas, B1 at El Crater) reached at least similar distances to the initially higher material (A4–A5 at Las Isletas and B2–B3 at El Crater). These observations altogether support a plug-flow-like model where shearing is concentrated at the base. The bulk of the mass above this basal layer is able to travel and spread without suffering bulk simple shear.

This basal lubricating layer is inferred to be the pumice-rich A1 unit under Las Isletas avalanche, and the hydrothermal clay-rich B1 unit under El Crater avalanche. Both share the common characteristic of being rheologically separated from the rest of the mass, as shown by the sharp transition they make with the overlying units, and both are extremely rich in fine material, which makes them ideal candidates for a more ductile behavior. Indeed, these powder/ash-rich units have a lower porosity and will show higher pore pressures that, in turn, will make them easier to liquefy/fluidize under applied stress.

At Las Isletas, the rounding of pumice compared to their original state in the Apoyo ignimbrite suggests that basal A1 may have undergone intense shearing, as such, a plug-flow-like transport requires.

We, thus, propose that, in both cases, lubricating layers are able to explain spreading and thinning of the avalanches until they came to rest.

Substratum incorporation

Unlike the Ollagüe DAD (Clavero et al. 2005), there is no evidence that El Crater and Las Isletas avalanches incorporated significant substrata by erosion. Basal erosion, rip-off mechanisms or bulldozing are not observed at Mombacho. Probably, one explanation for such substrata incorporation at Ollagüe is that a majority of its collapsing materials were composed of solid lava blocks (i.e., low matrix content), which have very high abrasion/erosion power. In addition, it is possible that high porosity in a dominantly blocky avalanche may favor substrate incorporation. At Ollagüe, lubrication could have occurred when sufficient substrate was incorporated at the base. Mombacho's collapses, on the other hand, both initially involved significant proportions of fine and soft materials (Apoyo ignimbrite A3 and clays from hydrothermal alteration in B2a–B1), which have poor abrasive capacities and, probably, lubricated the mass before it could erode substrata.

Preservation of original gross stratigraphical sequences

We have shown that, like other volcanic and nonvolcanic DADs such as those observed at Ollagüe (Clavero et al. 2005), Vesuvius, Elm and Goldau, Silver Reef, Gros Ventre, Sherman, and Martinez (see Shaller 1991), the initial gross stratigraphic sequences in both Las Isletas and El Crater are preserved. At Las Isletas, the initial material sequence was an alternation of lava/tephra above the Apoyo ignimbrite unit itself, chronologically positioned above the Las Sierras deposit. The lithological sequence after run-out is indeed the same except for the scoria/lava alternation, which separated into two units, lava blocks being above scoria and finer material. Similarly, at El Crater, the original sequence follows an order from top to bottom of less altered superficial lavas/tephras to extremely hydrothermally altered materials, which overall remains unchanged after avalanche run-out, apart from the lava/scoria succession. Thus, we conclude that to remobilize and generally preserve the order of such sequences, we can only invoke a nonturbulent translational transport that is devoid of significant large-scale mixing. In some cases, we also showed that smaller-scale portions of scoria deposits have preserved their initial configuration. These features probably belonged to satellite cones present on the precollapse surface.

Deformation

In terms of internal and superficial structures, both El Crater and Las Isletas DADs show normal faults generally oriented perpendicular to flow, and hummocks, both of which testify to extensional dynamics during avalanche flow. Such extensional features have already been described at Socompa (van Wyk de Vries et al. 2001), Parinacota (Clavero et al. 2002), and Ollagüe (Clavero et al. 2005) and form while the rock mass is thinning and laterally spreading. A phase of extension and spreading can be followed by compression upon arrival of the rock mass onto confining, flatter or up-slope topography. Accordingly, hummocks will form during the extensional phase and remain on the avalanche surface after suffering compression. In the latter case, they may then show elongations dominantly perpendicular to transport direction (e.g., Mt Shasta, Crandell et al. 1984; Parinacota, Clavero et al. 2002) or coalesce/thrust (Parinacota, Clavero et al. 2002). This, however, is clearly not the case at Mombacho, where hummocks are circular or elongated mostly parallel to transport (El Crater) or lacking dominant orientation (Las Isletas); in both cases, hummock trains suggest a varying flow-parallel direction, and hummocks are separated from one another, implying that compression was absent or insufficient to generate compound units. Thus, where in other avalanches, hummock formation may have later been strongly complicated by subsequent confinement or arrival onto topographic barriers, at El Crater and Las Isletas, they mostly recorded extension.

At Las Isletas and El Crater, normal faults tend to concentrate in proximal to central zones and progressively disappear toward distal zones, replaced by inter-hummock topographic depressions. This transformation is more complete at Las Isletas where few normal faults remain compared to El Crater deposit, and the deeper depressions exhumed the basal unit.

Unlike at Socompa and Ollagüe, however, no evidence of thrust or imbricate structures has been observed in Mombacho DADs. At Socompa, thrust faults appear in western zones, where the moving rock mass was required to go upslope, causing it to slow down at the front and suffer compression (van Wyk de Vries et al. 2001). In contrast, at Mombacho, substratum (Apoyo ignimbrite S2) shows regular and gentle (3°) slope both at Las Isletas and El Crater, allowing avalanches to spread horizontally on obstacle-free slide planes. At Ollagüe, compressive folds and faults affect, in particular, the incorporated substratum (Clavero et al. 2005). At Mombacho, the major basal units in both avalanches (A3 and B1) are unstratified, unsorted, and do not allow structural characterization. However, as the surface records only extensional spreading, the base, as

well as experiencing simple shear, must also have experienced a horizontal stretching. Mombacho's avalanches did not suffer compression during run-out and, possibly, freely spread until driving forces were too low for them to continue. This interpretation is supported by a simple observation that can be made for both avalanche deposits: The distal regions can be approximated in both cases to circular areas of similar diameters (best circular approximation, Fig. 4), which implies an isotropic spreading and thinning until stoppage. Accordingly, the centers of both circles should roughly represent the centers of gravity of the debris mass, which allows us to evaluate apparent coefficients of friction of $H/L=0.185$ for Las Isletas and $H/L=0.178$ for El Crater. The latter assumption requires that these represent the center of gravity. This is valid at El Crater where the deposit thickness is uniform; however, at Las Isletas the profile is distally raised, and the center of gravity may be somewhat closer to the distal regions (i.e., H/L slightly lower than 0.185).

Impact marks, jigsaw cracks, and clastic dykes

Hackly textures on the face of avalanche blocks have been described at Mt. St Helens (Komorowski et al. 1991), at Shiveluch (Belousov et al. 1999), at Parinacota (Clavero et al. 2002), and at Ollagüe (Clavero et al. 2005) and are thought to testify to block–block impacts during transport. In both El Crater and Las Isletas DADs, such textures were not observed, which indicates they probably did not interact violently with each other. Altogether, this reinforces the idea that the majority of materials involved suffered extension during horizontal transport and run-out, with internal blocks drifting apart from each other instead of colliding. Jigsaw cracks and clastic dykes are absent or uncommon in both deposits. We suggest that jigsaw cracking and impact marks may be produced predominantly in compression by block shocking and fracturing. The lack of clastic dykes can relate to lack of compression as well, which does not produce sufficient local overpressure to generate intrusion of fine particles through the moving mass. We nevertheless insist that the absence of such compressive features in these deposits does not in any way preclude compression and violent block-to-block interactions during the initial phases of collapse. Block angularity in debris avalanche deposits could well result from initial breakage as materials are compressed during transfer of vertical to horizontal forces. Smaller-scale hackly textures covering blocks in other avalanche deposits could, in turn, testify to block intershocking after initial fragmentation and during transport and run-out because of compressional waves generated by confinement or topographic obstacles.

Avalanche geometry

Both Las Isletas and El Crater DADs display spoon-like shapes in plan view and single-lobe distal fronts. Las Isletas shows slight heterogeneities (side-wings) that can relate to topographic variations or avalanche overflow. Accordingly, the presence of a small dacitic dome (Cerro Posintepe) in the western limits and the entrance of the moving mass into a different transport medium (Lake Nicaragua) in the eastern zones may have precluded free spreading at both sites. Alternatively, during the initial collapse stage and after primary confinement of the avalanche between the two amphitheater scarps, the progressively lower scar walls may have allowed overflow on both sides.

El Crater DAD shows a quite constant thickness from proximal to distal regions, whereas Las Isletas has a slightly raised distal profile. We can compare the uniform profile of El Crater avalanche deposit to the eastern zones of Socompa avalanche where the travel path was devoid of topographic barriers. In contrast, Las Isletas profile relates to that of Ollagüe where distal hummocky regions are thicker, especially where the avalanche entered the salt-rich and water-saturated Salar de Carcote. In both cases (Las Isletas and Ollagüe), the avalanche may have prematurely decelerated because of water (Lake Nicaragua) or extremely ductile medium (Salar de Carcote), which absorbed some of the rock mass kinetic energy. Such strong deceleration would indeed cause frontal material accumulation (hence, the distally raised profiles) and form thrust/imbricate structures at least at the base. As said previously, while such structures are described at Ollagüe, they do not appear at Las Isletas. This could be because the avalanche reacted by spreading more laterally, hence, the transport parallel zones observed in-between hummock trains (Fig. 4). A compression phase may have been overprinted by a latter extensional relaxation of the piled up avalanche front, or perhaps, this phase may be hidden under Lake Nicaragua.

Mobility

In terms of mobility, Las Isletas and El Crater avalanches both traveled ~12 km, and if the inferred collapse height for both is 1,345 m, then their respective apparent friction H/L is similar and approximates to 0.11. However, if we consider that Mombacho had a higher summit (above 1,500 m) before El Crater collapse (as drawn on photo Fig. 2), then the apparent friction coefficient H/L rises slightly to 0.12. The inferred failure plane for Las Isletas collapse did not propagate to the summit, and the uppermost portion of the current amphitheater is probably a better estimate of fall height. This would suggest a slightly increased mobility for Las Isletas avalanche (0.11

vs 0.12 for El Crater). In addition, if the run-out of Las Isletas avalanche was reduced by its entrance into Lake Nicaragua, then its actual friction coefficient may have been even lower. Even so, both avalanche deposits have comparable H/L (0.11–0.12) despite involving different failure mechanisms and some different materials. These H/L values do not differ from most volcanic and non-volcanic debris avalanches of similar volumes (Siebert 1984; Siebert et al. 1987; Shaller 1991), implying that they are not unusually mobile avalanches for their size.

Conclusions

We provide two examples of volcanic debris avalanches that have traveled over a nearly flat topography, with little terrain irregularity. This has allowed us to compare the structures and morphology of the deposits of two contrasting failure modes and to assess their differences and similarities in transport mechanisms. Figure 11 provides a schematic sequence of events that characterize the development of lithological units in a developing avalanche.

El Crater and Las Isletas avalanche deposits were studied in detail in terms of lithologies, structures, and geometries. Both show similarities when considering the depositional surface (Apoyo ignimbrite: gentle slopes, devoid of significant heterogeneities), the lack of associated magmatic activity, the lack of significant water contents, the capacity to preserve initial stratigraphic sequences, the presence of fine and ductile lubricating layers (A3 basal pumice-rich unit at Las Isletas and B3 basal extremely altered unit at El Crater) that contributed to reduced friction during transport. Both exclusively display extensional features such as normal faults, hummocks, boudinage structures, and the lack of evidence of inter-block collisions.

In contrast, the avalanches differ in that they came from very different scar geometries, shallow and u-shaped at Las Isletas, deep and bowl-shaped at El Crater; they show different hummock sizes, hummock distributions, different fault patterns, and involve different lithologies and potential lubricating layers.







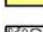




We also distinguish two different mechanisms for provoking flank failure, which confirm previous hypotheses made by van Wyk de Vries and Francis (1997) on Mombacho. We go further to show that, in each case, a different lithological distribution was involved by the contrasting failure geometries, which caused different structural styles. However, both produced a basal layer that was responsible for the low-friction sliding of the mass and the extensional structures observed. Thus, while materials were different, the general form of each deposit and its run-out were similar.

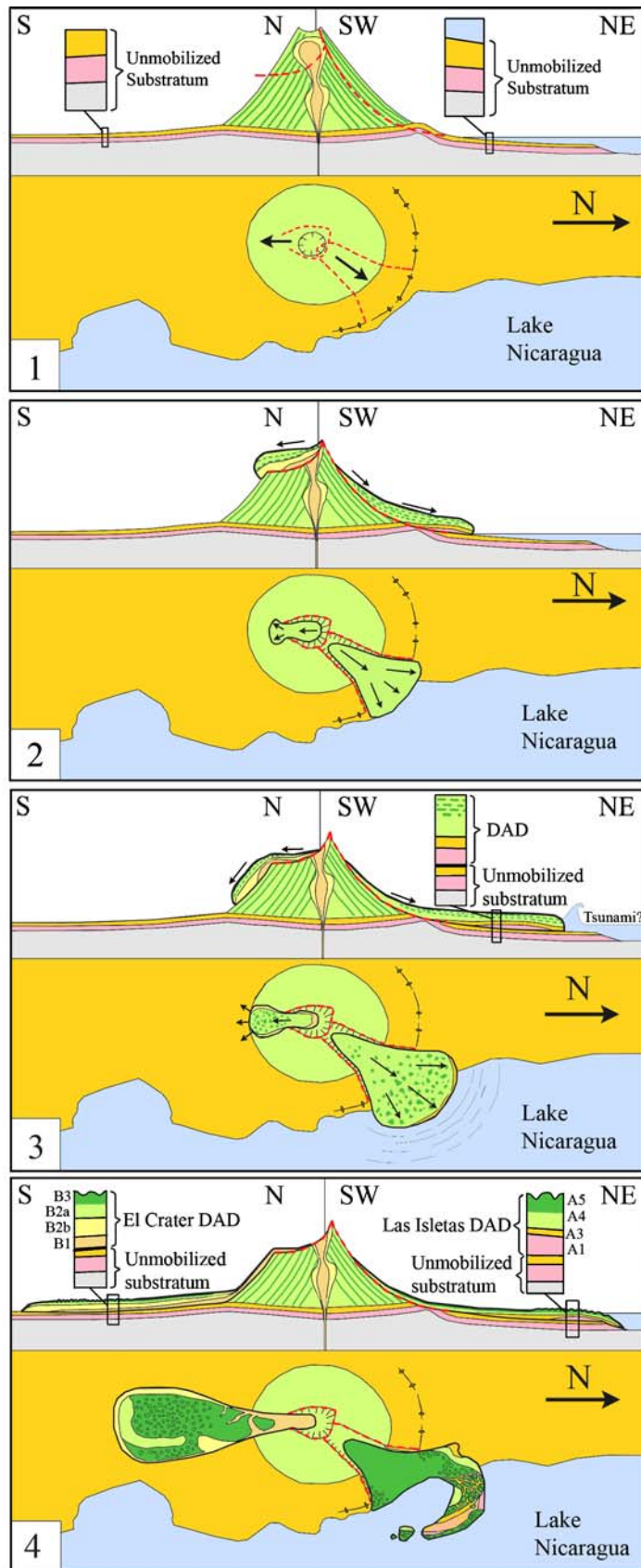
Fig. 11 Simplified sketches of the origin and evolution of lithologies in El Crater and Las Isletas avalanches. For comparison, Las Isletas and El Crater avalanches are represented at the same time. 1 Flank failure stage: At Las Isletas, the failure plan cuts through the underlying substratum (Apoyo and Las Sierras deposits) and, at El Crater, the deeper failure plan cuts through the hydrothermal system. Mombacho's original deposit sequences are alternating lava flows and tephra layers. 2 Primary avalanche stage: At both Las Isletas and El Crater, competent lava flows suffer stretching and boudinage. Fine matrix fills the gaps between blocks. Las Isletas avalanches uses the Apoyo substratum as lubricating layer, whereas El Crater avalanche takes advantage of the clay-rich hydrothermally altered layers for lubrication. 3 Segregation between competent lava blocks and softer tephra layers occurs in both avalanches. Blocks tend to rise upward or finer (fragmented?) tephra tends to fill the voids created by boudinage and, thus, migrates downward. In both cases, the lack of important topography allows for free lateral spreading. Nevertheless, Las Isletas avalanche entered Lake Nicaragua and may have generated a tsunami and lost some frontal velocity. 4 Material separation has now generated the typical bimodal matrix-rich and block-rich sequence, and both avalanches continue their thinning process, generating extensional horsts and grabens (hummocks) on their surface. Depending on material type and size, hummocks will vary in height and width. At Las Isletas, only the thicker, raised distal regions emerge and create the peninsula

We conclude that the geometry of the failure surface and the characteristics of initial material involved in massive flank collapses need not necessarily play important roles in transport and run-out as long as some basal lubricating layer can be formed at the base. The depositional surface, on the other hand, shows significant control over internal and superficial structure formation. At Mombacho, the lack of topographic variation allowed the avalanches to express fully the extensional dynamics during their spreading and thinning. Nevertheless, at Las Isletas, the entry of the mobile mass into Lake Nicaragua may have caused premature deceleration. In this way, Las Isletas DAD acquired a slightly distally raised profile, which differs from the uniform El Crater DAD profile.

Preserved gross stratigraphy, the absence of roll-over in both DADs, show that the rock mass slid without rotational or turbulent components. These observations and the lack of evidence supporting shearing in the uppermost portions of the deposits support a brittle plug-flow model, where the major fraction of a moving avalanche slides and thins on top of a highly sheared lubricated and/or fluidized basal layer. In addition, if stratovolcanoes are often alternating sequences of competent lava units and tephra initially, when they suffer flank collapse, the materials involved will often separate into two units: one which is block-rich and one which is matrix rich. Thus, the upper units do not stay completely “in place” as a plug flow model would suggest, their original layering suffers modifications. For us, three mechanisms are able to explain this phenomenon

- Simple passive or dynamic fragmentation (Davies et al. 1999; Davies and McSaveney 2002; Smith et al. 2006)

-  Tertiary basement
-  Las Sierras unit
-  Apoyo ignimbrite
-  Alternation between lava flows (dark green) and tephra (light green)
-  Extremely altered material
-  Altered material
-  Hummocks
-  Anticline fold
-  Failure plane
-  Topographic scar
-  Lake



can be concentrated at the base of the moving rock mass, hence, preferentially break lower fractions and cause the formation of a grossly bimodal deposit. Matrix fractions in both avalanches may have formed partly by fragmentation during collapse from the imposed overload (passive fragmentation) or by continuous violent interactions during transport (active dynamic fragmentation). The latter mechanism is inferred to be absent, however, in the bulk of the horizontal transport, as neither blocks nor matrix particles show evidence of violent collisions (e.g., hackly textures, conchoidal fracture surfaces). Active fragmentation would, thus, have to occur predominantly during the initial collapse stages at Mombacho. The latter mechanism, however, has mostly been investigated at the base of block-glides (e.g., Waikaremoana landslide, Davies et al. 2006) and not yet in granular avalanches.

- Competent lavas suffer boudinage and are separated into blocks, whereas finer particles tend to fill the voids in-between, generating a general downward migration of smaller materials.
- Blocks and, in general, larger rock fragments can migrate upward when submitted to vibrations caused by the collapse and transport of large volumes of rock as suggested by Savage and Lun (1988). This hypothesis seems confirmed at Las Isletas where allochthonous avalanche blocks are found within ancient cinder cone scoria layers (Fig. 5f) and further implies that, during avalanche, emplacement fragments can cross horizontal layers vertically without totally disrupting them. In other words, particle migration in moving rock flows is not opposed to preservation of former stratification.

In nature, these different mechanisms may all affect the moving rock mass at different times: During collapse, violent loading can cause fragmentation when vertical forces progressively gain their horizontal component, whereas separation processes (upward or downward migration) may take place during the bulk of the horizontal transport phase.

Finally, the lack of significant substratum incorporation in Las Isletas and El Crater is probably related to the early involvement of the lubricating basal layers, preventing the more solid, blocky fractions of the rock mass from eroding depositional surfaces.

Acknowledgment The authors thank Wilfried Strauch for the great assistance provided and INETER for supplying aerial photographs and maps. Thanks to Mario Carmelo Attubato for his assistance in mapping and collecting data at Las Isletas. The project was financed by the EU Alfa project CentralRisk. The authors also wish to thank Tim Davies and Stuart Dunning for their careful reviews.

References

- Ablay G, Hurlimann M (2000) Evolution of the north flank of Tenerife by recurrent giant landslides. *J Volcanol Geotherm Res* 103:135–159
- Belousov A, Belousova M, Voight B (1999) Multiple edifice failures, debris avalanches and associated eruptions in the Holocene history of Shiveluch volcano, Kamchatka, Russia. *Bull Volcanol* 61:324–342
- Borgia A, Ferrari L, Pasquarè G (1992) Importance of gravitational spreading in the tectonic and volcanic evolution of Mount Etna. *Nature* 357:231–235
- Borgia A, van Wyk de Vries B (2003) The volcano–tectonic evolution of Concepcion, Nicaragua. *Bull Volcanol* 65:248–266
- Bray (1977) Pleistocene volcanism and glaciation initiation. *Science* 197:251–254
- Carrasco-Nuñez G, Vallance JW, Rose WI (1993) A voluminous avalanche-induced lahar from Citlaltepetl volcano, Mexico: implications for hazard assessment. *J Volcanol Geotherm Res* 59:35–46
- Cecchi E, van Wyk de Vries B, Lavest JM (2004) Flank spreading and collapse of weak-cored volcanoes. *Bull Volcanol* 67:72–91
- Clavero JE, Sparks RSJ, Huppert HE (2002) Geological constraints on the emplacement mechanism of the Parinacota avalanche, northern Chile. *Bull Volcano* 64:40–54
- Clavero JE, Polanco E, Godoy E, Aguilar G, Sparks S, van Wyk de Vries B, Pérez de Arce C, Matthews S (2005) Substrata influence in the transport and emplacement mechanisms of the Ollagüe debris avalanche (Northern Chile). *Acto Vulcanol* 16:31–48
- Crandell DR, Miller CD, Glicken H, Christiansen RL, Newhall CG (1984) Catastrophic debris avalanche from ancestral Mount Shasta Volcano, California. *Geology* 12:143–146
- Davies TRH, McSaveney MJ (2002) Dynamic simulation of the motion of fragmenting rock avalanches. *Can Geotech J* 39:789–798
- Davies TRH, McSaveney MJ, Hodgson KA (1999) A fragmentation-spreading model for long run-out rock avalanches. *Can Geotech J* 36:1096–1110
- Davies TRH, McSaveney MJ, Beetham RD (2006) Rapid block glides—slide-surface fragmentation in New Zealand’s Waikaremoana landslide. *Q J Eng Geol Hydrogeol* 39:115–129
- Day SJ (1996) Hydrothermal pore fluid pressure and the stability of porous, permeable volcano. In: McGuire WJ, Jones AP, Neuberg J (eds) *Volcano instability on the Earth and other planets*. London, Geological Society Special Publication 110, pp 77–93
- Day SJ, Carracedo JC, Guillou H, Gravestock P (1999) Recent structural evolution of the Cumbre Vieja volcano, La Palma, Canary Islands: volcanic rift zone reconfiguration as a precursor to volcano flank instability. *J Volcanol Geotherm Res* 94:135–167
- Donnadieu F, Merle O (1998) Experiments on the indentation process during cryptodome intrusions: new insights into Mount St. Helens deformation. *Geology* 26:79–82
- Donnadieu F, Merle O, Besson JC (2001) Volcanic edifice stability during cryptodome intrusion. *Bull Volcanol* 63:61–72
- Dunning SA (2006) The grain-size distribution of rock-avalanches deposits in valley-confined settings. *Ital J Eng Geol Environ* 1:117–121
- Dunning SA, Rosser NJ, Petley DN, Massey CR (2006) Formation and failure of the Tsaticchu landslide dam, Bhutan. *Landslides* 3:107–113
- Elsworth D, Day SJ (1999) Flank collapse triggered by intrusion: the Canarian and Cape Verde Archipelagoes. *J Volcanol Geotherm Res* 94:323–340
- Elsworth D, Voight B (1995) Dike intrusion as a trigger for large earthquakes and the failure of volcano flanks. *J Geophys Res* 100:6005–6024

- Firth C, Stewart I, McGuire WJ, Kershaw S, Vita-Finzi C (1996) Coastal elevation changes in eastern Sicily; implications for volcano instability at Mount Etna. In: McGuire WJ, Jones AP, Neuberg J (eds) *Volcano instability on the Earth and other planets*. London, Geological Society Special Publication 110, pp 153–167
- Frank D (1983) Origin, distribution, and rapid removal of hydrothermally formed clay at Mount Baker, US Geological Survey Professional Paper, Washington, 1022-B, p 31
- Girard G, van Wyk de Vries B (2005) The Managua Graben and Las Sierras-Masaya volcanic complex (Nicaragua); pull-apart localization by an intrusive complex: results from analogue modeling. *J Volcanol Geotherm Res* 144:37–57 DOI [10.1016/j.jvolgeores.2004.11.016](https://doi.org/10.1016/j.jvolgeores.2004.11.016)
- Glicken H (1991) Sedimentary architecture of large volcanic-debris avalanches. In: Fisher RV, Smith GA (eds) *Sedimentation in volcanic settings*, SEPM Spec Pub 45:99–106
- Glicken H, Voight B, Janda RJ (1981) Rockslide–debris avalanche of May 18, 1980, Mount St. Helens volcano. IAVCEI Symp Arc Volc, Tokyo and Hakone, QE521.5A12, pp 109–110
- Gorshkov GS (1959) Gigantic eruption of the Volcano Bezymianny. *Bull Volcanol* 20:77–109
- Hürlimann M, Turon E, Marti J (1999) Large landslides triggered by caldera collapse events in Tenerife, Canary Islands. *Phys Chem Earth* 24:921–924
- Iverson RM, Reid ME, La Husen RG (1997) Debris-flow mobilization from landslides. *Annu Rev Earth Planet Sci* 25:85–138
- Komorowski JC, Glicken H, Sheridan MF (1991) Secondary electron imagery of microcracks and hackly fractures in sand-size clasts from the 1980 Mount St. Helens debris-avalanche deposits, implications for particle-particle interactions. *Geology* 19:261–264
- Lagmay AMF, van Wyk de Vries B, Kerle N, Pyle DM (2000) Volcano instability induced by strike-slip faulting. *Bull Volcanol* 62:331–346
- Lopez DL, Williams ST (1993) Catastrophic volcanic collapse: relation to hydrothermal processes. *Science* 260:1794–1796
- McGuire WJ (1996) Volcano instability: a review of contemporary themes. In: McGuire WJ, Jones AP, Neuberg J (eds) *Volcano instability on the Earth and other planets*. London, Geological Society Special Publication 110, pp 1–23
- McGuire WJ, Pullen AD, Saunders SJ (1990) Recent dyke-induced large-scale block movement at Mount Etna and potential slope failure. *Nature* 343:357–359
- McGuire WJ, Stewart LS, Saunders SJ (1997) Intra-volcanic rifting at Mount Etna in the context of regional tectonics. *Acta Vulcanol* 9:147–156
- Mooser F, Meyer-Abich H, McBirney AR (1958) Catalogue of the active volcanoes of the world, Part VI. International Volcanological Association, Napoli, Italy, p 35
- Pollet N, Schneider JL (2004) Dynamic disintegration processes accompanying transport of the Holocene Flims sturzström (Swiss Alps). *Earth Planet Sci Lett* 221:433–448
- Reid ME, Sisson TW, Brien DL (2001) Volcano collapse promoted by hydrothermal alteration and edifice shape, Mount Rainier, Washington. *Geology* 29:779–782
- Richards JP, Villeneuve M (2001) The Llullaillaco volcano, north-western Argentina: construction by Pleistocene volcanism and destruction by edifice collapse. *J Volcanol Geotherm Res* 105:77–105
- Savage SB, Lun CKK (1988) Particle size segregation in inclined chute flow of dry cohesionless granular solids. *J Fluid Mech* 189:311–335
- Shaller PJ (1991) Analysis and implications of large Martian and terrestrial landslides. PhD thesis, California Institute of Technology, California
- Siebe C, Komorowski J-C, Sheridan MF (1992) Morphology and emplacement of an unusual debris-avalanche deposit at Jocotitlan volcano, central Mexico. *Bull Volcanol* 54:573–589
- Siebert L (1984) Large volcanic debris avalanches: characteristics of source areas, deposits, and associated eruptions. *J Volcanol Geotherm Res* 22:163–197
- Siebert L, Glicken H, Ui T (1987) Volcanic hazards from Bezymianny- and Bandaï-type eruptions. *Bull Volcanol* 49:435–459
- Smith GM, Davies TR, McSaveney MJ, Bell DH (2006) The Acheron rock avalanche, Canterbury, New Zealand—morphology and dynamics. *Landslides* 3:62–72
- Stoopes GR, Sheridan MF (1992) Giant debris avalanches from the Colima volcanic complex, Mexico: implication for long-run-out landslides (>100 km). *Geology* 20:299–302
- Ui T (1972) Recent Volcanism in Masaya–Granada area, Nicaragua. *Bull Volcanol* 36:174–190
- Ui T (1983) Volcanic dry avalanche deposits. Identification and comparison with nonvolcanic debris stream deposits. *J Volcanol Geotherm Res* 18:135–150
- Vallance JW, Scott KM (1997) The Osceola mud-flow from Mount Rainier: Sedimentology and hazard implications of a huge clay-rich debris-flow. *Geol Soc Am Bull* 109:143–163
- Van Benmelen (1949) The geology of Indonesia, vol. IA. General geology of Indonesia and adjacent archipelagos, 732 pp, vol. IB (portfolio), 60 pp
- van Wyk de Vries B (1993) Tectonics and magma evolution of Nicaraguan volcanic systems. PhD thesis, Milton Keynes, The Open University, UK
- van Wyk de Vries B, Merle O (1996a) The effect of volcanic constructs on rift fault patterns. *Geology* 24:643–646
- van Wyk de Vries B, Borgia A (1996b) The role of basement in volcano deformation. In: McGuire WJ, Jones AP, Neuberg J (eds) *Volcano instability on the Earth and other planets*. London, Geological Society Special Publication 110, pp 95–110
- van Wyk de Vries B, Francis PW (1997) Catastrophic collapse at statovolcanoes induced by gradual volcano spreading. *Nature* 387:387–390
- van Wyk de Vries B, Kerle N, Petley D (2000) Sector collapse forming at Casita volcano, Nicaragua. *Geology* 28:167–170
- van Wyk de Vries B, Self S, Francis PW, Keszthelyi L (2001) A gravitational spreading origin for the Socompa debris avalanche. *J Volcanol Geotherm Res* 105:225–247
- van Wyk de Vries B, Oehler JF, Smellie J (2003) Gravitational tectonics at Mt Haddington, an Antarctic submarine/subglacial volcano. EGS-AGU-EUG Joint Assembly, Nice, France, 6–11 April 2003
- van Wyk de Vries B (2004) Report on 3rd field visit to James Ross Island. Br Antarctic Surv Prelim Report, 5 pp
- Vidal N, Merle O (2000) Reactivation of basement faults beneath volcanoes: a new model of flank collapse. *J Volcanol Geotherm Res* 99:9–26
- Voight B, Elsworth D (1997) Failure of volcano slopes. *Geotechnique* 47:1–31
- Voight B, Glicken H, Janda RJ, Douglass PM (1981) Catastrophic rockslide avalanche of May 18. In: Lipman PW, Mullineaux DR (eds) *The 1980 eruptions of Mount St. Helens*, US Geological Survey Professional Paper, Washington, DC 1250, pp 347–377
- Voight B, Janda RJ, Glicken H, Douglass PM (1983) Nature and mechanics of the Mount St Helens rockslide avalanche of 18 May 1980. *Geotechnique* 33:243–273